Major Project

Dissertation on

"WASTE HEAT RECOVERY OF NAVAL SHIP GAS TURBINE EXHAUST USING TRANSCRITICAL CO_2 CYCLE"

Submitted to Delhi Technological University in partial fulfilment of the requirement for the award of Degree of

Master of Technology

In

Thermal Engineering

PRADEEP KUMAR BARNWAL

2K13/THE/17

UNDER THE SUPERVISION OF

Dr. K. Manjunath

Asst. Professor

Department Of Mechanical Engineering

Delhi Technological University

Delhi-110042

Department of Mechanical Engineering
Delhi Technological University
(Formerly Delhi College of engineering)
Bawana Road, Delhi-110042

JULY 2015

STUDENTS DECLARATION

I **Pradeep Kumar Barnwal**, hereby certify that the work which is being presented in the major project-II entitled "**Waste heat recovery of a naval ships gas turbine exhaust using Transcritical CO_2 cycle"**is submitted in the partial fulfilment of the requirements for the degree of **M.Tech** at **Delhi Technological University** is an authentic record of my own work carried under the supervision of **Dr. K. Manjunath**. I have not submitted the matter embodied in this major project-2 for the award of any other degree. Also it has not been directly copied from any source without giving its proper reference.

Pradeep Kumar Barnwal

M.tech (Thermal Engineering)

2K13/THE/17

CERTIFICATE

DELHI TECHNOLOGICAL UNIVERSITY
(Formerly DELHI COLLEGE OF ENGINEERING)

Date:-_____

This is to certify that report entitled **"WASTE HEAT RECOVERY OF A NAVAL SHIP GAS TURBINE EXHAUST USING TRANSCRITICAL CO_2 CYCLE"** by PRADEEP KUMAR BARNWAL is the requirement of the partial fulfilment for the award of Degree of **Master of Technology (M.Tech)** in **Thermal Engineering** at **Delhi Technological University**. This work was completed under my supervision and guidance. He has completed his work with utmost sincerity and diligence. The work embodied in this project has not been submitted for the award of any other degree to the best of my knowledge.

SUPERVISIOR
DR. K. MANJUNATH
Asst. Professor
Department of Mechanical Engineering
DELHI TECHNOLOGICAL UNIVERSITY

ACKNOWLEDGEMENT

First of all, I would like to express my gratitude to God for giving me ideas and strengths to make my dreams true and accomplish this thesis.

To achieve success in any work, guidance plays an important role. It makes us put right amount of energy in the right direction and at right time to obtain the desired result. Express my sincere gratitude to my guide, **Dr. K. Manjunath**, Asst. Professor, Mechanical Engineering Department for giving valuable guidance during the course of this work, for his ever encouraging and timely moral support. His enormous knowledge always helped me unconditionally to solve various problems.

I am greatly thankful to **DR. R. S. MISHRA**, Professor and Head, Mechanical Engineering Department, Delhi Technological University, for his encouragement and inspiration for execution of the this work. I express my feelings of thanks to the entire faculty and staff, Department of Mechanical Engineering, Delhi Technological University, Delhi for their help, inspiration and moral support, which went a long way in the successful completion of my report work.

PRADEEP KUMAR BARNWAL

(Roll No-2K13/THE/17)

ABSTRACT

Common power cycles discard a large portion of useful energy into the environment via exhaust gases. Through the use of cascade bottoming cycles, this wasted energy may be utilized for power generation. Heat transfer between cycles occurs through a waste heat recovery heat exchanger. To maximize heat exchange, a transcritical working fluid is used in the Rankine bottoming cycle to better match the heating curve of the sensible heat source. Carbon dioxide is selected as the working fluid because it possesses a relatively low critical temperature which makes it attractive for low temperature waste heat applications. In contrast to many other working fluids, carbon dioxide is inert, abundant, non-flammable, and presents negligible environmental impact. The purpose of this study is to quantify the performance of the transcritical bottoming cycle and the combined cycle as a whole by altering system parameters by using commercially available 'EES' software to gain insight for future research in the field of waste heat recovery. This thesis also includes the economic analysis of system by calculating the cost of system power output annually.

Parametric analysis and exergy analysis are conducted to examine the effects of thermodynamic parameters on the cycle performance and exergy destruction in each component. The thermodynamic parameters of the transcritical CO2 power cycle is optimized with exergy efficiency as an objective function by means 'EES' software under the given waste heat condition. It is shown that the key thermodynamic parameters, such as turbine inlet pressure, turbine inlet temperature, environment temperature and exhaust temperature from naval ships gas turbine have significant effects on the performance of the transcritical CO2 power cycle and exergy destruction in each component.

CONTENTS

LIST OF FIGURES

LIST OF TABLES

NOMENCLATURE

H	Enthalpy
S	Entropy
T	Temperature
T_{ref}	Reference Temperature
T_{add}	Average temperature of heat addition
T_{reject}	Average temperature of heat rejection
K	Ratio of specific heats
E	Exergy
M	Mass flow rate
R_P	Pressure ratio
TIT	Turbine inlet temperature
$V_{DOMESTIC}$	Volumetric flow rate of domestic water
BTU	British Thermal Unit
WHRHX	Waste Heat Recovery heat exchanger
IHX	Internal Heat Exchanger
ODP	Ozone Depletion Potential
ORC	Organic Rankine Cycle
GWP	Global Warming Potential
U	Overall heat transfer Coefficient
A	Heat Exchanger surface area
EES	Engineering Equation Solver
CO_2	Carbon Dioxide
ΔT_{HOT}	WHRHX hot side temperature difference
ΔT_{COLD}	WHRHX cold side temperature difference

ΔP	Relative Pressure Loss
dS	Entropy Change
η_1	First law efficiency
η_2	Second law efficiency
η_R	Recuperator Effectiveness
η_C	Compressor isentropic efficiency
η_{1CC}	Combined cycle first law efficiency
E_D	Component Exergy Destruction
W_{net}	Net Power Output
$\dot{Q}$	Heat Transfer Rate

Subscripts

1,2,……15	State 1,2,…..15
i, inlet	Inlet state
e, exit	Exit state
B	Brayton
R	Rankine
Comb	Combustion
Net	Net amount
Reg	Regenerator

Chapter 1

1. INTRODUCTION

1.1 MOTIVATION

Energy security, economic development and environment protection are not well balanced today and the energy demands still closely connected to the economic growth. At the same time, the increasing consumption of fossil fuels has led to more and more environment problems such as global warming, ozone depletion and atmospheric pollution. Fossil fuels still play the dominant role in energy resources worldwide, accounting for 77% of the increasing energy demand 2007-2030. Furthermore, along with the fast Development of industry, energy shortages and blackouts have appeared more and more frequently all over the world. Due to all these reasons, utilizing low-grade waste heat for energy production has attracted more and more attention for its potential in reducing the fossil fuel consumption.

The most commonly investigated cycles in low-grade heat source and waste heat utilizations today are Organic Rankine Cycles (ORCs) and Kalinga cycle (binary fluids and fluid mixtures). When utilizing low grade waste heat, the traditional steam Rankine cycle does not give satisfactory performance due to its low thermal efficiency and large volume flows; and thus so called Organic Rankine cycle (ORCs) have been proposed. These cycle use organic substances as working fluid system consist of at least five major component: evaporator, turbine, pump, condenser and working fluid. To make an equal comparison with the CO_2 process later, a regenerator is also included in the current calculation.

According to waste heat recovery report by U.S. DOE, industrial processes in the United States consumes approximately 35 quadrilion BTU(Quads) of energy per year [1]. This amount is about 30% of total energy consumed in the United States. This reports also estimates that around 25-50% of that energy is lost to waste heats [1]. The report categorizes the waste heat based on the temperature of the waste products. The three waste heat groups are: low, medium, high temperature. Table 1 defines the temperature range for each source based on limited samples of industrial application. Table 1 also shows the amount of waste

heat and work potential of each waste heat group [1]. The waste heat and work potential is based on the reference temperature of 25^{o} C.

	Temperature Range °C	Waste Heat (1055 trillion joules per year) 25ºC *Reference*	150ºC *Reference*	Work Potential (1055 trillion joules per year) 25ºC *Reference*
Low	< 230	903	37	287
Med	230-650	466	130	216
High	>650	108	89	86
Total	-	1478	256	589

Table 1.1: Yearly national unrecovered waste heat [1]

This data indicates that low temperature heat source results in 60 % of total waste heat source. It is estimated that 305.95 trillion KJ per year or 33% of this low temperature heat can be recaptured into useful works. Low temperature heat source recovery presents the largest opportunity to recover among other discarded heat.

1.2 PINCH PROBLEM

A common method to convert waste heat to useful work is through a Combined cycle or Bottoming cycle. The Bottoming cycle may be a gas power or vapour power system in which heat is transfer between cycles via heat exchanger (HX). A popular type of heat exchanger is the heat recovery steam generator (HRSG) which combines an economiser, an evaporator and a superheater [2]. Marrero et al. [3] use the steam product of a HRSG to power a bottoming cycle. Utilizing a HRSG, combined power cycles capable of achieving 60 % thermal efficiency have been constructed [4]. In a HRSG a hot Exhaust gases heats another working fluid from a liquid to a two phase mixture, a saturated vapour or superheated vapour.

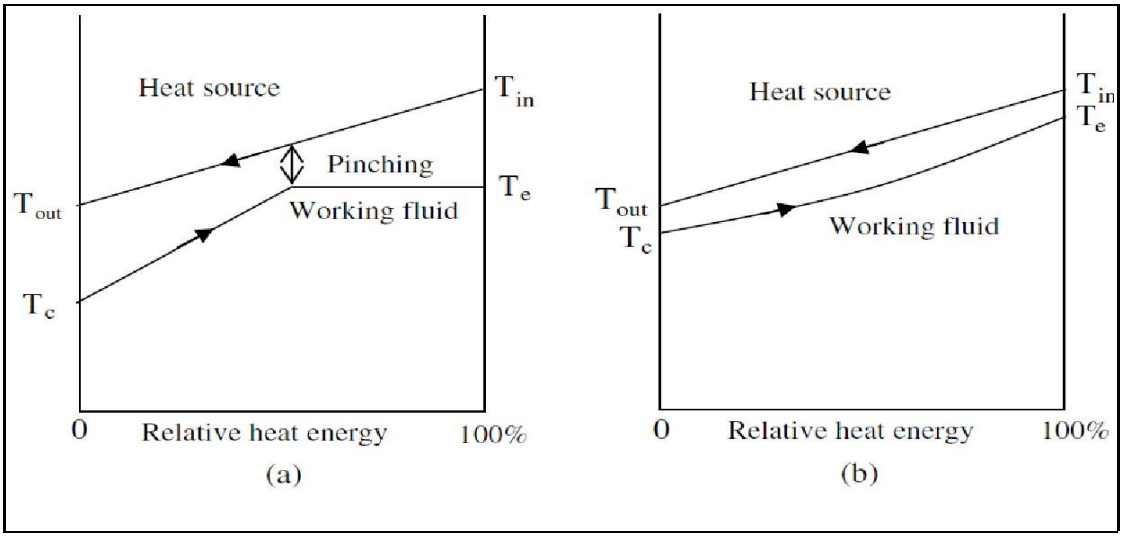

Figure 1.1: Schematic representation chart of the heat transfer between waste heat and working fluid in the high temperature main heat exchanger. (a) ORC cycle; (b) CO2 transcritical power cycle [5].

Figure 1.1(a) shows an example of the cooling curve in a HRSG [5]. Heat is supplied to the working fluid as it goes through a phase transition. Remember that temperature is constant of working fluid during phase change. The working fluid undergoes sensible cooling during which temperature continuously decreases. Pinch point is the minimum temperature difference between heat source and working fluid as shown in figure 1.1(a). The existence of Pinch point causes two desirable effects:

1. Heat transfer between two fluids is proportional to temperature difference between them. The temperature difference at the pinch point reduces the effectiveness of heat exchanger. As a result, the minimum heat transfer occurs at the pinch point. This reduces the total amount of heat that can be supplied to the working fluid.

2. In order to prevent the reversal direction of heat transfer, the average temperature difference between the fluids must be larger than the necessary with a single phase fluid (refer to figure 1.1 (a)). These relative temperature difference on both side of the Pinch point would result in more Entropy production within the heat exchanger.

A proposed solution to the pinch problem is to use a single phase working fluid that more closely matches the heat source fluid temperature profile [5]. This would result in

sensible cooling or a “temperature glide” in the heat exchanger. Supercritical fluids remain in a single phase but compared to gases, have smaller specific volumes and better transport properties [6]. A system using a supercritical working fluid therefore has a relatively low volume to power ratio [7]. This low volume to power ratio requires smaller system components to achieve the same power output [8]. It is proposed by many authors to use supercritical fluids for application to waste heat recovery [5],[9],[10],[11],[12],[13].

Figure 1.1 (b) shows a schematic of behaviour of supercritical working fluid in a heat exchanger with a sensible heat source. This study will investigate the performance of Rankine cycle using Transcritical CO_2cycle for waste heat recovery.

1.3 Working fluid selection

There are many thermo-physical properties that should be considered when selected working fluid for utilising the energy into low grade heat source and waste heat. For instances, the critical temperature and critical pressure indicates whether the cycle run as a Transcritical or Supercritical cycle, the possibility for condensing and the system working pressure respectively.

Carbon Dioxide has favourable characteristics for the following reasons:

- Moderate critical pressure of 7.4 MPa.
- Relative low critical temperature (31^{o}C) is well suited for low temperature heat source.
- Abundance, non-flammability, non-toxic etc. [10].
- It is environment-friendly with an ozone depletion potential (ODP) of zero and a global warming potential (GWP) of 1 over 100 years.[14]
- Its thermo-physical properties are well known even in the supercritical area.
- It is compatible with the standard materials and lubricants and is not harmful to the environment.
- It has potentially favourable thermodynamics and transports properties.

- limited research and information available for CO_2 power cycle with low temperature heat source . [11]

Table 1.2 list critical properties and environmental properties of common refrigerants that can be used as working fluid.

Name	Refrigerant Number	Formula	Critical Temperature[a]C	Critical Pressure[a] MPa	Ozone Depletion Potential[b]	Global Warming Potential[b]
Ammonia	R-717	NH_3	133	11.2	0	0
Carbon Dioxide	R-744	CO_2	31	7.4	0	1
Water	R-718	H_2O	374	22.1	0	<1
Propane	R-290	$CH_3CH_2CH_3$	97	4.3	0	~0
Butane	R-600a	$CH_3CH_2CH_2CH_3$	152	3.8	0	~0
	R-22	$CHClF_2$	96	5	0.055	1500

Table 1.2: Critical and environmental properties of common refrigerants. [11].

Compared to other working fluid listed in Table 1.2, Carbon Dioxide has low critical temperature (31^oC) and relatively high critical pressure (7.4 MPa). Due to low critical temperature, even a low grade heat source can give a Transcritical cycle whose “gliding” temperature profile can provide a better match to heat source temperature glide than other working fluid.

Chapter 2

2. LITERATURE REVIEW

According to many papers, studies on the behaviour of carbon dioxide in low temperature transcritical power cycles are not extensively reported [5],[10],[11]. To better understand the behaviour of these types of systems, more research is required. In the interest of waste heat recovery, some researchers analyse various configurations of CO_2 bottoming cycles or organic Rankine bottoming cycles. Other researchers directly compare carbon dioxide power cycles to organic Rankine cycles (ORC). Some of the sources of heat in these papers include solar, combustion exhaust gasses, and other generalized industrial waste heat sources. A second law analysis of CO_2 Transcritical cycle with variations in topping cycle parameters has not been exhaustively reported. Therefore, the necessity for a second law analysis of the "full system" behaviour is a major motivation for this study.

2.1 Organic Rankine Cycles

Roy et al. [15] conduct a theoretical analysis of bottoming ORC operating with R12, R134a, and R123 as the working fluid. The goal of the study is to determine which of the three working fluids investigated is best suited for application to waste heat recovery. The selection of each organic working fluid is based on the slope of the saturated vapour curve for each. The vertically sloped or "isentropic fluid" is R12. The positively sloped or "dry fluid" is R123. The negatively sloped or "wet fluid" is R123a. The naming convention is due to the turbine exit state: a superheated gas with a "dry fluid", a saturated vapour with an "isentropic fluid", and a liquid-vapour with a "wet fluid". An example of a "wet fluid" is shown in Figure 11. The waste heat is based on data from the NTPC Kahalgaon plant. Exhaust gas at 140 °C and 312 kg/s is used to heat the bottoming cycle. The bottoming cycle in the analysis consists of a HRSG, a turbine, a condenser, and a pump. The system energetic efficiency, exergetic efficiency, and work output are maximized for each working fluid by varying the turbine inlet pressure in the ORC. A summary of the results is given in Table 3. In the application of waste heat power generation, maximum power production is the primary design criteria. Of the three working fluids, R123 has the highest power production. The author concludes that the gradient of the saturated vapour line on a temperature versus

entropy plot affects the efficiency of the system. Also, the lower pinch point temperature in the R123 cycle results in the highest exergetic efficiency [15].

Velez et al. [16] compare the maximum efficiency of an ORC using common refrigerants with a maximum source temperature of 150 °C. The organic fluids in the study are R134a, R152, R290, R718, R600, and R600a. The analysis is performed by the process simulator HYSYS®. The authors use the energetic efficiency to evaluate the working fluids' performance in the cycle. The input parameters are the turbine inlet temperature and the pressure ratio of the cycle. The results indicate that for the "wet fluids" R152a, R290, and R718, the energetic efficiency increases with an increase in turbine inlet temperature. For the "dry fluids" R600 and R600a, the energetic efficiency decreases with an increase in turbine inlet temperature. For the "isentropic fluid" R134a,

Working Fluid Parameters/outputs			
Parameters	R-12	R-123	R134a
Power generated (MW)	9.13	19.09	11.71
First law efficiency (%)	12.09	25.30	15.53
Second law efficiency (%)	30.01	64.40	37.80
Mass flow rate (kg/s)	541.8	341.2	417.8
Condenser water flow rate (kg/s)	1980	1712	1899
Pinch point (°C)	19.00	5.00	25.00

Table 2.1: Summary of results from [15]

the energetic efficiency is unaffected by variation in turbine inlet temperature. In every case, the energetic efficiency increases with an increase in cycle pressure ratio. In a direct comparison of the six organic fluids tested, R152 achieves the highest energetic efficiency.

Vaja et al. [17] investigate a combined cycle with an internal combustion engine (ICE) as the topping cycle with a bottoming ORC. The two heat sources in the study for the bottoming cycle are the engine coolant and the exhaust gas. Three configurations of the ORC are analysed. Figure 2.1 shows a schematic representation of the three setups.

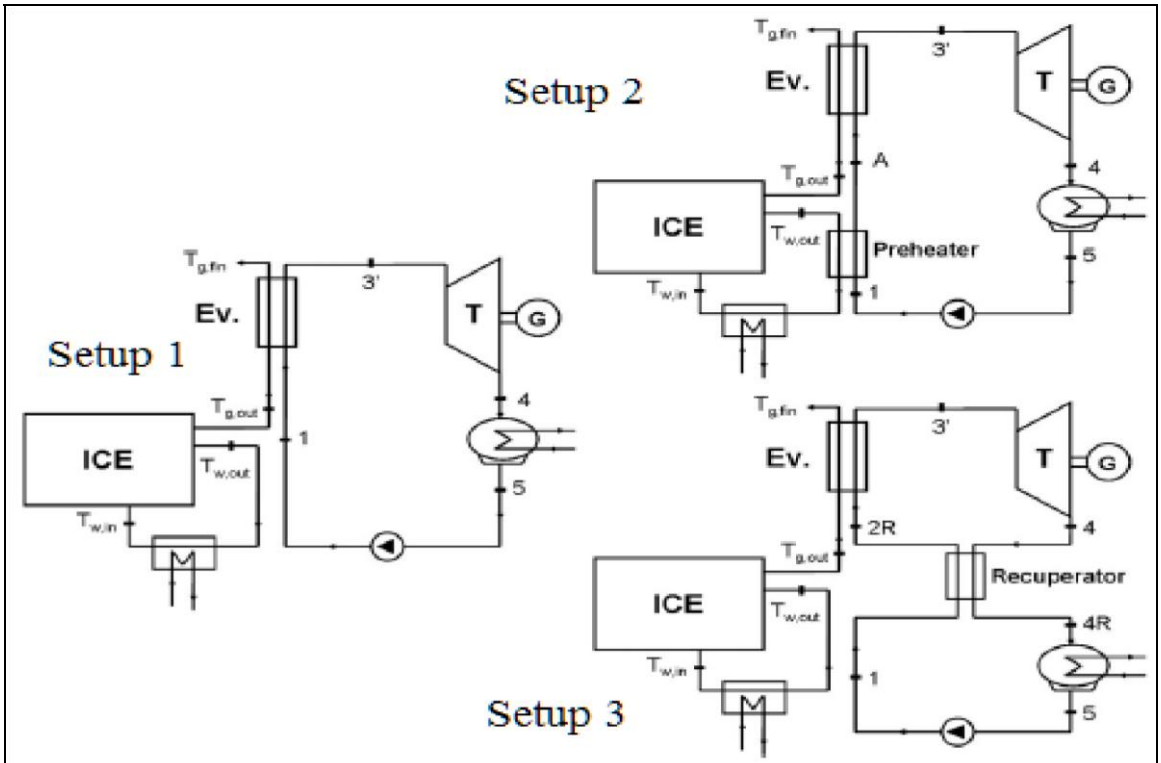

Figure 2.1 Schematic of setups used by Vajaet. al [18]

In all cases the bottoming cycle contains a turbine, a condenser, and a pump. The differences between the three setups are the following:

- *Setup 1*: A simple Rankine cycle heated by the ICE exhaust gas.

- *Setup 2*: The same as *Setup 1* with an included Rankine cycle preheater attached to the ICE coolant.

- *Setup 3*: The same as *Setup 1* with an included IHX in the Rankine cycle. Each configuration is analysed with R11, R134a, and benzene as the bottoming cycle working fluid. Therefore, a total of nine unique systems are analysed. The analysis assumes exhaust gas at 470 °C with a flow rate of 4.35 kg/s and engine coolant at 90 °C at a flow rate of 24 kg/s. Table 2.2 shows the combined cycle energetic efficiency for each setup with each respective working fluid. The top portion shows the combined cycle efficiency while the bottom portion shows the relative improvement over the baseline efficiency of the internal combustion engine alone. The efficiency of the standalone internal combustion engine is estimated to be 41.8 %.

Vaja et al. [17] analyse the regenerated cycle only with benzene because benzene is the only "dry fluid" of the three being investigated. Furthermore, these "dry fluids" are the type most commonly used in commerce. Benzene achieves the highest 1st Law efficiency for *Setup 1* and *Setup 2*. The analysis also reveals that utilizing preheat or regeneration (at least with benzene) is more efficient than a simple Rankine bottoming cycle alone.

Combined Cycle Efficiency			
	Simple cycle	Simple cycle with preheat	Regenerated cycle
Benzene	46.6%	47.1%	47.1%
R-11	45.8%	46.3%	-
R-134a	43.8%	44.5%	-
Relative Improvement over Baseline			
Benzene	11.4%	12.6%	12.8%
R-11	9.5%	10.8%	-
R-134a	4.8%	6.5%	-

Table 2.2: Cycle efficiencies [17]

2.2 Comparison of CO_2 to Other Working Fluids

Guo et al. [18] present a theoretical analysis of natural and conventional working fluids in a regenerated Rankine cycle with a geothermal heat source. The temperature range of the heat source is 80-120°C. To define a reference temperature for heat addition and rejection in the heat exchangers, the thermodynamic mean temperatures are implemented and are defined as:

$$\overline{T}_{add} = \frac{h_e - h_i}{s_e - s_i}, \quad \text{for heat addition} \tag{1}$$

$$\overline{T}_{reject} = \frac{h_i - h_e}{s_i - s_e}, \quad \text{for heat rejection} \tag{2}$$

where “h” is the state enthalpy and “s” is the state entropy with the “i”subscript indicating the device inlet state and the “e” subscript indicating the device exit state.

CO_2 is the baseline for comparison to the other fluids. A pinch-point temperature difference of 5 °C is chosen. It observe that the pinch point in the gas heater for transcritical CO_2 occurs at the outlet state, i.e. the turbine inlet state [18].

Table 2.3 shows a comparison of the results [18] for each working fluid tested with a thermal source temperature of 100 °C. R115 achieves the highest thermal efficiency. R218 generates the highest net power which is likely due to having the highest pressure ratio and volumetric expansion ratio. R218 also has the highest heat exchanger overall thermal conductance (UA), resulting in the lowest heat source temperature of 41.8°C.

Fluid	Heat source H/X exit temperature (°C)	Thermal Efficiency (%)	Net power (kW)	UA (kW/K)	Volumetric expansion ratio	Pressure ratio
CO_2	45.7	6.45	1.38	5.87	1.62	1.84
R-115	63.2	9.37	1.37	3.90	4.63	3.52
R-41	42.5	6.99	1.59	6.90	1.92	2.16
R-218	41.8	7.48	1.73	7.57	8.25	4.41
R-170	49.9	6.99	1.38	5.98	1.87	1.93

Table 2.3: Summary of results [18]

In regard to the pinch problem, Chen et al. [5] compare an ORC using R123 to transcritical CO_2 power cycle. A regenerated Rankine cycle is used for both cycles with a minor difference being the transcritical cycle contains a gas heater and the ORC contains an evaporator. The authors speculate that for a cycle using waste heat at moderate temperature (80-200 °C) as a heat source, the best efficiency and highest power output is obtained when the working fluid temperature profile can match the temperature profile of the heat source [5]. The authors use the thermodynamic mean temperature for heat transfer in the heat exchangers. The analysis is performed with EES [19]. A comparison of the results for the transcritical CO_2 power cycle and the R123 ORC are provided in Table 2.4. The CO_2 has a turbine inlet temperature of 140 °C which is more than 55 °C above the turbine inlet temperature using R123. In addition, the exhaust gas temperature leaving the HX is 12.7 °C lower when using R123. This indicates that more heat is indeed extracted from the exhaust gas. The premise that transcritical CO_2 would more effectively capture heat from the exhaust gas appears to be confirmed. The only apparent drawback to using transcritical CO_2 is that a smaller expansion ratio must be used because of the relatively high condenser pressure required. Even with a smaller expansion ratio, the carbon dioxide cycle was able to achieve about a 1.2 % increase in power output versus R123.

Working fluid	Turbine inlet temperature (^oC)	Heat addition Pressure(bar)	Exhaust gas exit temperature(^oC)	Specific power output(KW/Kg)	Expansion ratio
CO_2	140	16	61.3	8.16	2.67
R123	84.4	5.3	74	8.06	6.91

Table 2.4: Summary of results [5]

Cayer et al, [20] compares CO_2, R125a, ethane in Transcritical power cycle. A simple Rankine cycle is analysed using industrial heat as a heat source with temperature 100^oC and mass flow rate 314.5 Kg/s. Turbine inlet temperature and turbine inlet pressure is the system inlet parameters. The analysis is done in 4 sections. The first two sections are an energy and exergy analysis, respectively. The third section is a finite size thermodynamic analysis which determines UA. The fourth and final section of the analysis determines the required surface area of each heat exchanger by using empirical approximations for the overall heat transfer coefficient, "U". Figure 2.2 shows the 1^{st} Law efficiency and specific net work, with CO_2 as the working fluid, plotted versus turbine inlet pressure (shown as maximum pressure) and the turbine inlet temperature (shown as T_{max}). As the turbine inlet temperature increases, both the thermal efficiency and the net specific work increase. It should be noted that as the turbine inlet temperature approaches the temperature of the thermal source (100 °C), the required heat exchanger surface area becomes impossibly large.

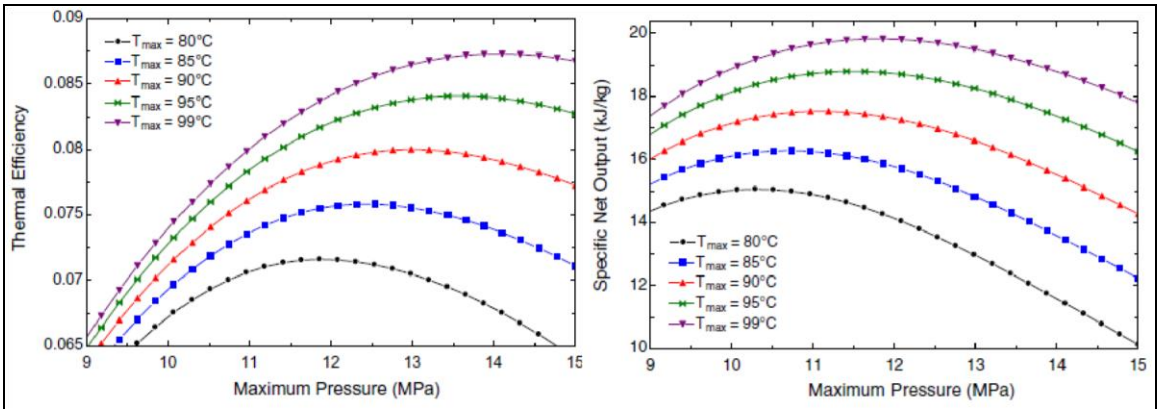

Figure 2.2 1st Law efficiency and net specific work versus turbine inlet temperature [20]

It can be concluded from the figure that it is impossible to maximize both the thermal efficiency and the net specific work simultaneously. It conclude that in application to waste heat recovery, focus should be on maximizing the net specific work rather than the thermal efficiency [21].

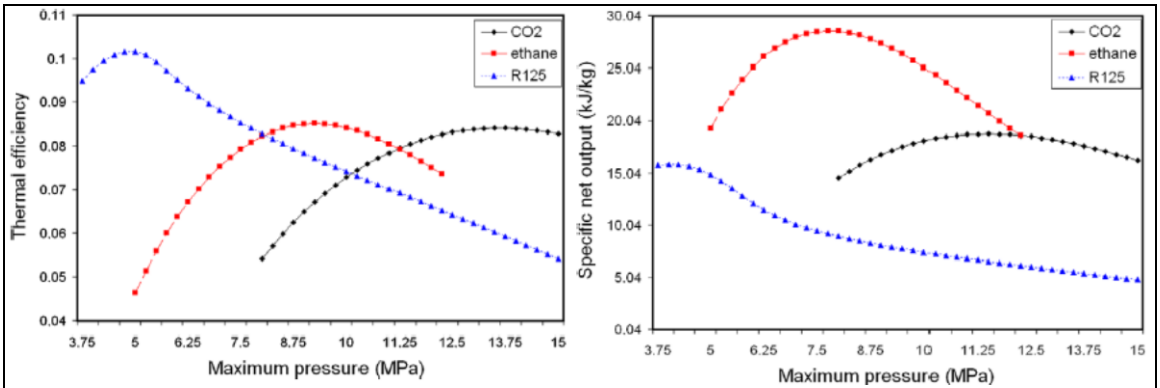

Figure 2.3 Thermal efficiency and net specific work versus fluid and TIP [20]

Figure 2.3 compares the thermal efficiencies and net specific works for all three working fluids evaluated versus turbine inlet pressure. R125 has the highest thermal efficiency of about 10 %. Ethane has the highest net specific work of about 29 kJ/kg. Although ethane has the highest net specific work, it is flammable and requires the largest "A" of the fluids sampled [20].

Chen et al. [21] compare R32 to CO_2 in a transcritical Rankine cycle utilizing low grade heat at temperatures ranging from 373-453 K (100-180 °C) . An energetic and

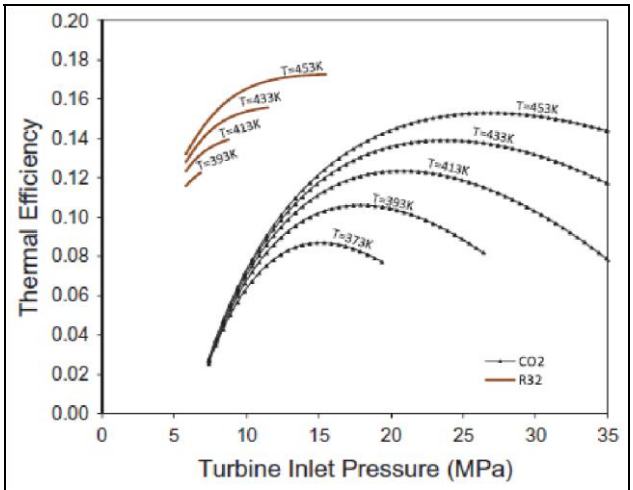

Figure 2.4 Thermal efficiency results [21]

exergetic analysis is performed. Figure 2.4 compares the thermal efficiencies of CO_2 and R32 at various turbine inlet temperatures and turbine inlet pressures. It is apparent that transcritical R32 achieves higher thermal efficiencies than transcritical CO_2 and at lower operating pressures. Despite the higher thermal efficiencies, R32 is rated "highly flammable" by the ECHA classification system. The high flammability of R32 prevents its use in applications where safety is the primary concern. The exergy distribution and 2nd Law efficiency for CO_2 is shown in Figure 2.5. The turbine inlet temperature is held constant at 433 K. The greatest source of exergy destruction within the cycle is the condenser. For a given turbine inlet temperature, the maximum exergetic efficiency and maximum net power occur at different pressures at the turbine inlet.

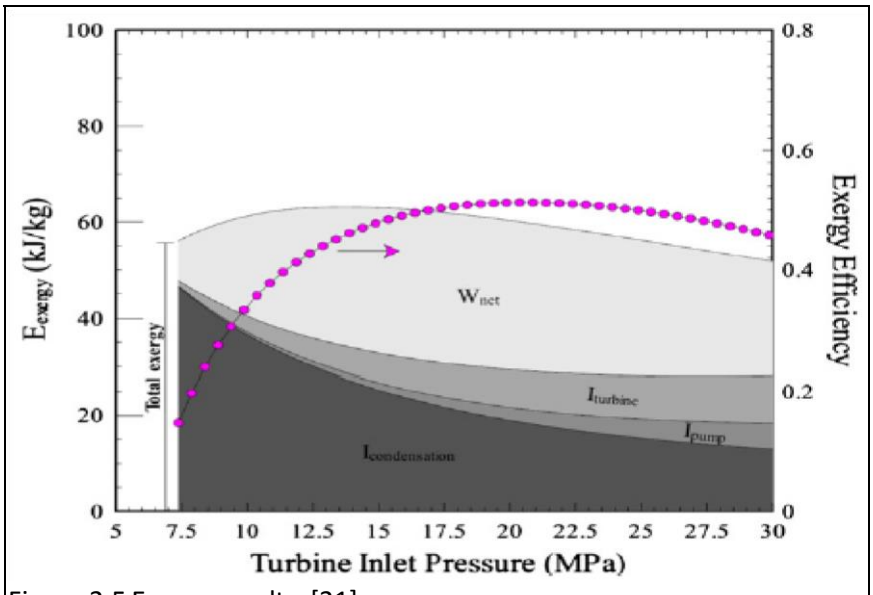

Figure 2.5 Exergy results [21]

2.3 Bottoming Cycles with CO_2

Persichilli et al. [9] describe a waste heat recovery power system developed by Echogen Power Systems LLC. The cycle is a recuperated Rankine cycle with supercritical CO_2 as the working fluid. The system is designed to use industrial process waste heat between 200 °C (473 K) and 540°C (813K). The system is scalable to produce 250-50,000 kW. A noted advantage of a supercritical system over a traditional ORC is the component miniaturization. A size comparison between the Echogen 10 MWe supercritical CO_2 turbine and an equivalent steam turbine is shown in Figure 7 [9].

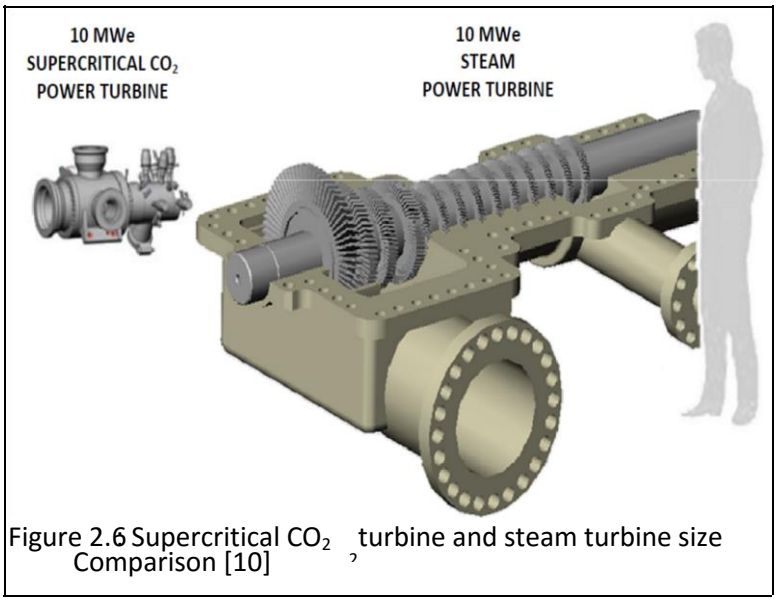

Figure 2.6 Supercritical CO_2 turbine and steam turbine size Comparison [10]

The authors also mention another advantage of using a supercritical working fluid instead of a subcritical working fluids is pinch point avoidance. It predict that the system can reduce the Levelized Cost of Electricity by 10-20 % with efficiencies up to 30 % [9].

Velez et. al. [11] conduct an analysis on a transcritical CO_2 power cycle with a low temperature heat source. An energy and exergy analysis, performed in HYSYS®, is conducted on a simple Rankine cycle and on a regenerated Rankine cycle. The input parameters are the turbine inlet temperature and the turbine inlet pressure.

	Parameter				
	TIT (°C)	TIP (bar)	Energetic Efficiency (%)	Exergetic Efficiency (%)	Net Specific Work (kJ/kg)
	150	141.0 [161.0]	9.8 [8.0]	48 [38]	18.1[18.0]
with IHX	120	124.0 [136.5]	7.3 [6.4]	46 [36]	12.6[12.5]
[without IHX]	90	106.0 [114.0]	4.8 [4.5]	43 [34]	7.7 [7.6]
	60	88.5 [92.5]	2.4 [2.5]	40 [30]	3.5 [3.4]

Table 2.5: Summary of results [11]

Table 2.5 shows the results obtained when the net specific work is maximized by varying the turbine inlet pressure for each selected temperature at the turbine inlet. The obvious benefit of increasing the turbine inlet temperature is an increase of the net specific work. The table also indicates that as the turbine inlet temperature increases, the pressure at the turbine inlet must increase to achieve the maximum net specific work [11].

Similarly to the behaviour observed [20], the authors notice there is no operation point that simultaneously produces maximum efficiency and maximum net specific work. In all cases analyzed, inclusion of an IHX increased the exergetic efficiency but had little effect on the net specific work.

To reduce fuel consumption in automotive applications, Chen et al. [22] proposes three system layouts to utilize ICE exhaust gas waste heat. The first design concept, named the Reversible Cycle, is illustrated in Figure 2.7. It is a redesign of the existing A/C cycle which can run in reverse as a transcritical power cycle when compartment cooling is not necessary. The gas heater pressure is set to 130 bar and the gas cooler pressure is set to 60 bar. The turbine inlet temperature is preset to 200 °C. Figure 8(b) shows the second cycle design concept which contains the existing A/C system with an added parallel power cycle. This setup, named the Auxiliary Power Unit (APU), can be used to produce electricity and heat when the ICE is idling or function as a Brayton cycle to convert waste heat into extra power. The heat source is the ICE exhaust gas.

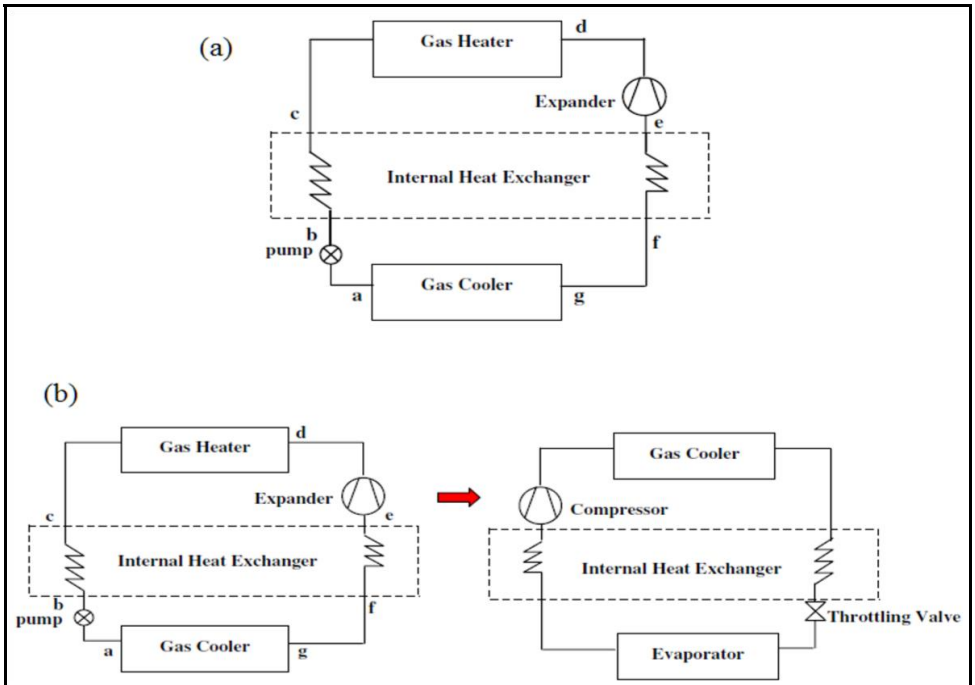

Figure 2.7 : First two setups used [22]

The APU is analyzed for two different operating scenarios. The first scenario operates as a transcritical cycle with the gas heater pressure set to 300 bar and the condenser pressure is set to 60 bar. The second scenario operates entirely in the supercritical region as a Brayton cycle with the gas heater pressure maintained at 300 bar and the gas cooler pressure raised to 100 bar. The turbine inlet temperature is increased to 350 °C. The third design concept layout, named the Combined Cycle, is illustrated in Figure 9. Internal heat exchangers are included in all setups with the intention of improving efficiencies.

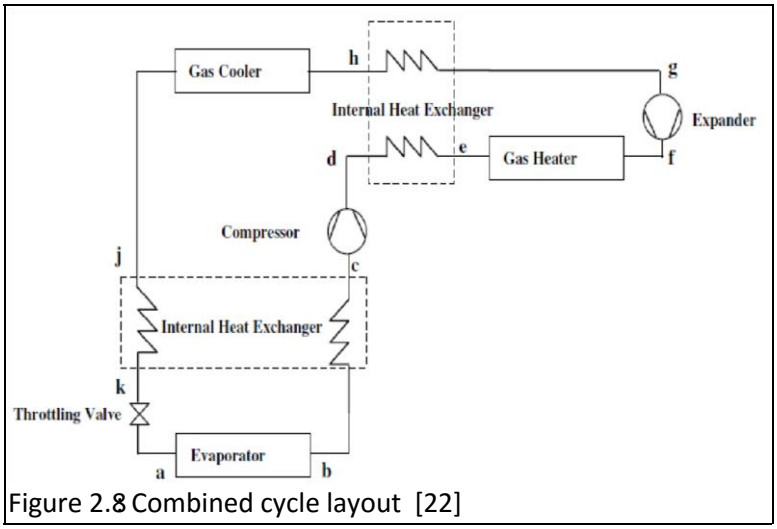

Figure 2.8 Combined cycle layout [22]

A summary of system parameters and results is provided in Table 2.5. For each setup, the thermal efficiency is calculated using an internal heat exchanger effectiveness of 60 % and 90 %. Note that the second heat addition pressure for the combined cycle represents the evaporator pressure. The table indicates the highest thermal efficiency is achieved by the reversible cycle with an internal heat exchanger effectiveness of 90 %. The configuration with the lowest thermal efficiency is the combined cycle with a recuperator effectiveness of 60%. Although the supercritical APU cycle appears to have a higher efficiency than the transcritical version, it should be noted that the pressure ratios and turbine inlet temperatures of the two cycles differ. The authors determine that even by varying the internal heat exchanger effectiveness, the Reversible Cycle always has the highest thermal efficiency [22].

Byung Chul Choi and Young Min Kim [23] performs a dual loop waste heat recovery power generation system that comprises an upper trilateral cycle and a lower organic Rankine cycle, in which discharged exhaust gas heat is recovered and re-used for propulsion power, was theoretically applied to an internal combustion engine for propulsion in a 6800 TEU container ship. The thermodynamic properties of this exhaust gas heat recovery system, which vary depending on the boundary temperature between the upper and lower cycles, were also investigated. The results confirmed that this dual loop exhaust gas heat recovery power generation system exhibited a maximum net output of 2069.8 kW, and a maximum system efficiency of 10.93% according to the first law of thermodynamics and a maximum system exergy efficiency of 58.77% according to the second law of thermodynamics. In this case, the energy and exergy efficiencies of the dual loop system were larger than those of the single loop trilateral cycle. Further, in the upper trilateral cycle, the volumetric expansion ratio of the turbine could be considerably reduced to an adequate level to be employed in the practical system. When this dual loop exhaust gas heat recovery power generation system was applied to the main engine of the container ship, which was actually in operation, a 2.824% improvement in propulsion efficiency was confirmed in comparison to the case of a base engine. This improvement in propulsion efficiency resulted in about 6.06% reduction in the specific fuel oil consumption and specific CO_2 emissions of the main engine during actual operation.

2.4 Economic analysis of Transcritical CO_2 cycle

Min-Hsiung Yang and Rong-Hua Yeh [24] investigate the economic optimization of a TRC system for the application of geothermal energy. An economic parameter of net power output index, which is the ratio of net power output to the total cost, is applied to optimize the TRC system using CO2, R41 and R125 as working fluids. The maximum net power output index and the corresponding optimal operating pressures are obtained and evaluated for the TRC system. Furthermore, the analyses of the corresponding averaged temperature differences in the heat exchangers on the optimal economic performances of the TRC system are carried out. The effects of geothermal temperatures on the thermodynamic and economic optimizations are also revealed. In both optimal economic and thermodynamic evaluations, R125 performs the most satisfactorily, followed by R41 and CO2 in the TRC system. In addition, the TRC system operated with CO2 has the largest averaged temperature difference in the heat exchangers and thus has potential in future application for lower-temperature heat resources. The highest working pressures obtained from economic optimization are always lower than those from thermodynamic optimization for CO2, R41, and R125 in the TRC system

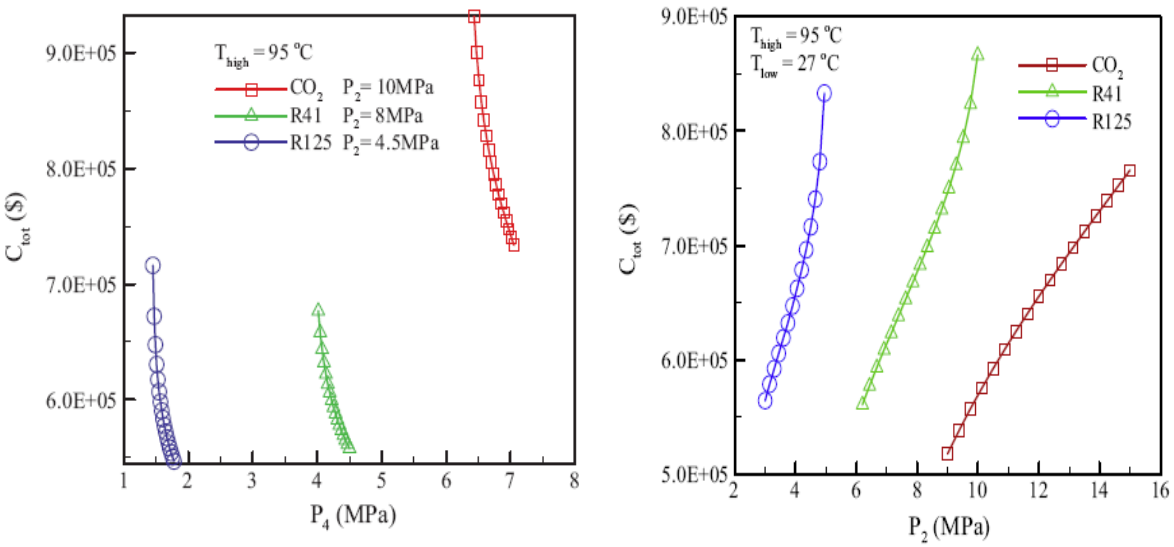

Figure 2.9 (a): Cost verses Pump inlet pressure , Figure 2.9 (b): Cost verses turbine inlet pressure

Figure 2.9: The effect of Pump inlet (a) and turbine inlet pressure (b) on total cost [24].

Farivar Fazelpour and Tatiana Morosuk [25] analyse a simple transcritical CO2 refrigeration machine from the perspectives of energetic, exergetic, economic and exergo economic analyses. Special attention has been paid to the transcritical cycle under hot climatic conditions. The main goal of this paper is to define the energy and cost efficient transcritical CO2 refrigeration machine, therefore the options for the structure and parametric improvements are discussed. Introducing the economizer as an auxiliary component for one-stage transcritical CO2 refrigeration machine helps us to decrease the total cost of the final product by approximately 14%.

Sylvain Quoilin, Sébastien Declaye, Bertrand F. Tchanche, Vincent Lemort [26] focused on the economic optimization of a small scale ORC in waste heat recovery application. A sizing model of the ORC is proposed, capable of predicting the cycle performance with different working fluids and different components sizes. The working fluids considered are R245fa, R123, n-butane, n-pentane and R1234yf and Solkatherm. Results indicate that, for the same fluid, the objective functions (economics profitability, thermodynamic efficiency) lead to different optimal working conditions in terms of evaporating temperature: the operating point for maximum power doesn't correspond to that of the minimum specific investment cost: The economical optimum is obtained for n-butane with a specific cost of 2136 V/kW, a net output power of 4.2 kW, and an overall efficiency of 4.47%, while the thermodynamic optimum is obtained for the same fluid with an overall efficiency of 5.22%. It is also noted that the two optimizations can even lead to the selection of a different working fluid.

Chapter 3

3. PURPOSE AND METHOLOGY

3.1 Purpose Statement

The purpose of statement is to analyse the performance of Transcritical CO_2 cycle and to calculate the performance of Combined Cycle as a whole by altering system parameters to get development efforts in the field of waste heat recovery and to gain insight for future research. These measurements will include energetic efficiency, exergetic efficiency, component wise irreversibility and economic analysis of system per KW power output.

3.2 System Description

The system analysed is a combined power cycle which consist of an Air Brayton topping cycle and a Transcritical CO_2 Rankine bottoming cycle. Assumptions for the system are the following:

1. Each component is considered as a steady-state steady-flow system.
2. The kinetic and potential energy changes are neglected.
3. The heat and friction losses are neglected.
4. All the heat exchanger are well insulated.
5. The effect of mass change in combustor are negligible.
6. Carbon Dioxide exits the condenser as saturated liquid.
7. Pinch point occurs at a side of the heat exchanger rather than the center due to the temperature glide condition shown in Figure 1(b).
8. The definition of “isentropic efficiency” is used to determine exit states of expansion and compression processes.
9. Internal geometry of the heat exchanger are such that the parametric temperature differences between inlets and outlets are possible.

10. The definition of “recuperator effectiveness” is a control parameter for the recuperator.

A schematic of the system layout is shown in figure 3.1. Each component of system is labelled along with associated intermediates states. Air is the working substance of Brayton topping cycle and Transcritical CO_2 is the working substance for Rankine bottoming cycle.

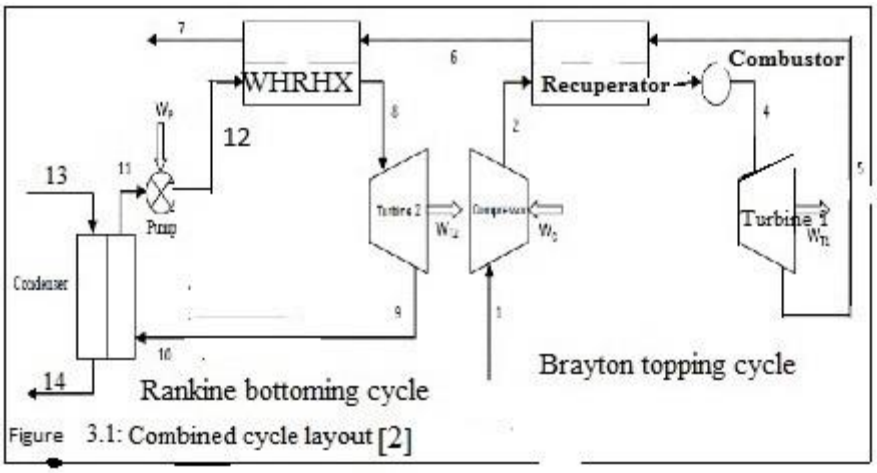

Figure 3.1: Combined cycle layout [2]

Air enters the compressor at ambient condition i.e. pressure is reference pressure (101.3KPa) and temperature is reference temperature (290 K). Air exits the compressor to the high pressure at state 2. Air then enters the cold stream side of recuperator where it is preheated by hot exhaust gas. The air then leaves the recuperator at state 3 and enters into combustor. Inside combustor, heat is supplied from the combustion of air with methane. Then exhaust gas leaves the combustor at state 4 and expands in turbine 1 . After expansion in turbine 1, the expanded exhaust gas enters the recuperator through hot stream side at state 5. The high temperature exhaust gas leaves the hot stream side of recuperator at state 6 and proceeds into the waste heat recovery heat exchanger(WHRHX) also known as Gas Heater. Within the WHRHX, heat is transferred from the Brayton cycle exhaust gas to the Carbon Dioxide in the Rankine cycle. The low temperature exhaust gas from the WHRHX at state 7 is discharge into the atmosphere.

Transcritical CO_2 enters the turbine 2 at state 8 where it is expanded between state 8 and 9. Between state 9 and 10, heat is rejected to cold steam side of internal heat exchanger (IHX). The CO_2after state 10 enters the condenser in which heat is rejected by domestic water at 40^oC. After exhaust from condenser , CO_2 enters the pump as saturated liquid at state 11. Next, CO_2 passes through the pump to the maximum pressure and leaves at state 12 and then

enters the Rankine side of WHRHX and the cycle is repeated. Water enters the condenser at atmospheric condition. If at some point during operation, the inlet temperature of cooling water exceeds critical temperature of Transcritical CO_2 i.e. 31^{o}C, the cycle would operate entirely in the supercritical region.

A temperature versus entropy diagram of the bottoming CO_2 cycle is shown in figure 3.2. The figure indicates actual states and isentropic states, for ex: state 9s is state after isentropic expansion and state 9 indicates actual expansion.

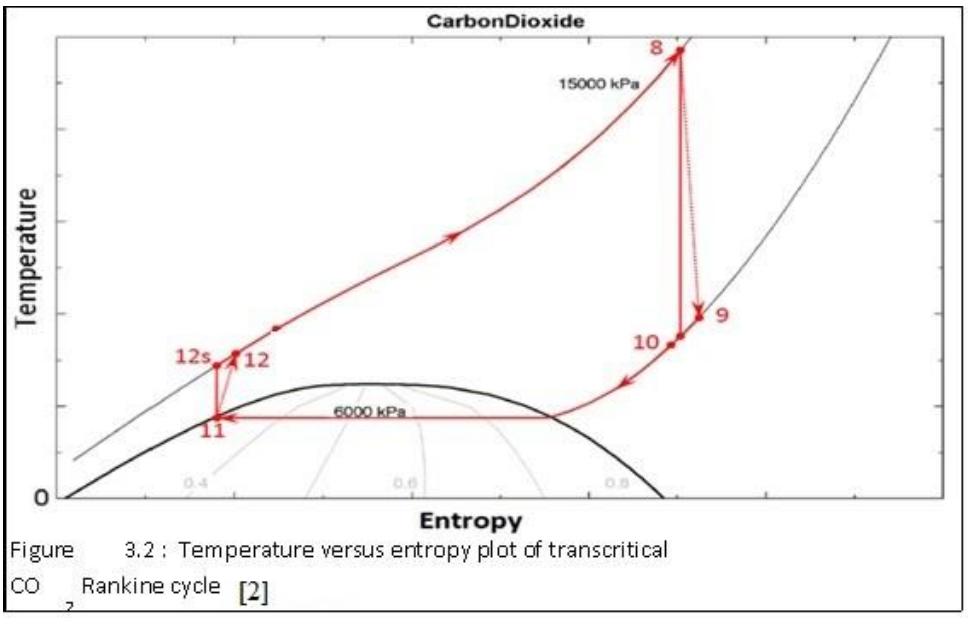

Figure 3.2 : Temperature versus entropy plot of transcritical CO_2 Rankine cycle [2]

It should be noted that pressure losses through the heat exchanger are not shown in the figure but will be included in the analysis.

3.3 Methodology of Analysis

A First Law and Second Law of Thermodynamics analysis will be conducted on the system using EES [19]. The thermodynamic properties for air are taken from the EES definition "Air" which is approximated as an ideal gas. Thermodynamic properties for CO_2 are taken from the EES definition "CarbonDioxide" which is valid for temperatures up to 1100 K and pressures up to 800 MPa. For "CarbonDioxide", the reference states for enthalpy and entropy are 290 K and 101.3 KPa [19].

The system has multiple control parameters.

3.3.1 Naval Ships Gas Turbine Exhaust Control Parameters

Typical gas turbine engine are less than 35 % thermally efficient at full power [27], and significantly less at partial power. Although diesel engine efficiency is more uniform across its operating power range, thermal efficiency typically does not exceed 45%. The engine exhaust stream is the primary pathway of engine waste heat, see Table 3.2. Recovering useful energy, in the form of electrical power, alternative heating and cooling, from engine exhaust waste heat would directly reduce system fuel consumption, increase available electric power and improve overall system efficiency by augmenting the power produced by the prime mover and enabling it to operate at a lower net power with lower net fuel consumption. Industrial gas turbines have achieved efficiencies—up to 60%—when waste heat from the gas turbine is recovered by a heat recovery system in a combined cycle configuration. Identification and development of a viable shipboard waste heat recovery system in this effort will provide reduced ship service electric power fuel consumption.

Typical marine gas turbine characteristics

Gas Turbine Type	**Exhaust Temperature(K)**	**Mass flow rate (Kg/s)**
501K17/34	733	15.422
LM2500	838.7	70.3
MT30	733.2	113.39
ETF40B	877	13.15
TF40B	900	13.6

Table 3.1: Typical marine gas turbine [27] Extracted from publicly available reference material

So, from table we can say that the range of Exhaust temperature of gas turbine is 860^{o}F to 1120^{o}F. If we change in ^{o}K, then range is 733 to 900 K . For simple analysis in EES, the exhaust temperature of gas turbine may be taken as 800 K.

3.3.2 System Control Parameters

Table 3.2 contains a list of system control parameters with associated minimum, maximum and nominal values. This section explains the rational for selecting the ranges of values. The minimum and maximum value of ambient temperature are taken from 5^{o}C to 30^{o}C which are comparable to most regions of U.S. throughout the year.

Input Parameters	Unit	Value		
		Minimum	Maximum	Nominal
Ambient/Reference Temperature	K	278	300	290
Brayton Turbine Inlet Temperature	K	1200	1500	1350 [2]
Rankine Cycle Maximum Pressure	KPa	10000	20000	15000 [5]
Brayton Cycle Pressure Ratio	-	3	19	16
Recuperator/IHX effectiveness	%	0.6	1	0.85 [3]
Brayton Compressure Isentropic Efficiency	%	0.75	1	0.9 [3]
Brayton turbine Isentropic Efficiency	%	0.70	1	0.9 [3]
WHRHX hot end temperature difference	K	8	18	12 [5]
WHRHX cold end temperature difference	K	10	30	22 [5]
Condenser Approach Temperature Difference	K	2	10	2
Recuperator Relative pressure loss	%	0	5	5

Combustor Relative Pressure loss	%	0	5	5
WHRHX Pressure loss	%	0	5	5
Condenser Relative Pressure loss	%	0	5	5
Gas turbine Exhaust Temperature	K	733	900	800 [27]
Rankine cycle Minimum Pressure	KPa	5000	8000	6000 [5]

Table 3.2: System input Parameters

The turbine inlet temperature is limited by current material restrictions. The maximum value of turbine inlet temperature in Brayton cycle is due to material limitation. Kehlhofer provides a maximum temperature limit of 1525 K for commonly available gas turbines[2].

.

The maximum brayton cycle pressure ratio is taken from the following equation for maximum work,

$$(\mathrm{Pr})\max = \left(\frac{T\max}{Tref}\right)^{\frac{k}{2(k-1)}} = \left(\frac{1500}{278}\right)^{\frac{1.4}{0.8}} \approx 19 \qquad (3)$$

Where T_{max} is the maximum turbine inlet temperature and T_{ref} is the reference or ambient temperature and k is the ratio of specific heats for air. It should be noted that Brayton cycle operates at high pressure ratio which includes: intercooling between the stages of compressor which reduces compressor work and reheat between stages of turbine to increase turbine work.

For the WHRHX, rather than pinch point the control parameter is the temperature difference between WHRHX inlet and outlet. Since the condenser exits is assumed to be saturated liquid, so the temperature difference used is the difference between state 13 and state 11. The need of this temperature difference because like the WHRHX, a value of zero would require an infinite heat exchanger surface area. This value is also chosen from similar way as above [5].

3.3.3 Evaluation Metrics

Some common thermodynamic analysis is done to evaluate and compare the system operating under different parametric conditions. The analysis includes the system first law efficiency, the system second law efficiency and component wise exergy destruction.

The first law efficiency is simply defined as:

$$\eta_1 = \frac{\dot{W}_{NET}}{\dot{Q}_{in}} \tag{4}$$

Where W_{NET} is the net power output and Q_{in} is the rate of heat transfer into the system. Brayton Cycle work is:

$$\left(\dot{W}_{NET}\right)_B = \left(\dot{W}_{T1} - \dot{W}_C\right) = \dot{m}_B\left(h_4 - h_5 - h_2 + h_1\right) \tag{5}$$

Where W_{T1} is Brayton turbine work and W_C is compressor work.

Rankine cycle work is:

$$\left(\dot{W}_{NET}\right)_R = \left(\dot{W}_{T2} - \dot{W}_P\right) = \dot{m}_R\left(h_8 - h_9 - h_{12} + h_{11}\right) \tag{6}$$

Where W_{T2} is the Rankine turbine work and W_P is pump work.

Combine Cycle work:

$$\left(\dot{W}_{NET}\right)_{CC} = \left(\dot{W}_{NET}\right)_B + \left(\dot{W}_{NET}\right)_R \tag{7}$$

The second law efficiency is defined as:

$$\eta_2 = \frac{Exergy_{used}}{Exergy_{\sup plied}} = \frac{\dot{W}_{NET}}{\dot{E}_{fuel}} = \frac{\dot{W}_{NET}}{\dot{W}_{NET} + \sum_j \dot{E}_D + \sum_k \dot{E}_{flow}} \quad (8)$$

Where "Exergy used" is net power output from equation (5) or (6), E_{fuel} is the exergy addition from fuel, $\sum_j \dot{E}_D$ is the sum of exergy destruction of each component. $\sum_k \dot{E}_{flow}$ is the net exergy flowing across the system.

Our goal of this study is to analyse the exergy destruction of each component of the system. Another analysis is to determine the minimum isentropic turbine efficiency in the Rankine cycle which results in a positive net power output.

The exergy at each point is calculated as:

$$e_i = (h_i - h_0) - T_o(s_i - s_o) \quad (9)$$

Where 0 state is corresponding to ambient condition.

3.3.4 Analysis Procedure

In this thesis, analysis of system is done in two section. In first section,analysis of Combined cycle is done in two parts, in first part analysis validates the air standard Brayton cycle using air as working substance and in second part analysis validates the Rankine Cycle using Transcritical CO_2 as a working substance. This analysis is sensitivity analysis of each input parameters. The parameter of need is evaluated over the range specified in table 11. All other input variables are set to their nominal values during analysis. The purpose of this section is to evaluate which parameter have the greatest influence of the selected figures of merits.

In second section, Economic analysis of system is done to evaluate the cost of each component, total installation cost and total running cost. The alternate cycle which produces domestic hot water is calculated under nominal parameter values. The performance and feasibility of the alternate system is discussed in chapter 4.

3.3.4.1 Component equations of Brayton Cycle:

Compressor:

The work done by compressor is:

$$\dot{W}_C = \dot{m}_B (h_2 - h_1) \tag{10}$$

Exergy destruction in compressor is:

$$(\dot{E}_D)_C = \dot{W}_C + \dot{m}_B (e_2 - e_1) \tag{11}$$

Entropy generation of compressor:

$$(S_{gen})_C = \frac{(\dot{E}_D)_C}{T_{ref}} \tag{12}$$

Recuperator:

Heat transfer in recuperator is:

$$\dot{Q}_B = \dot{m}_B (h_3 - h_2) \tag{13}$$

Exergy destruction in recuperator is:

$$(\dot{E}_D)_{reg} = \dot{m}_B (e_2 + e_5 - e_3 - e_6) \tag{14}$$

Entropy generation in recuperator:

$$(S_{gen})_{reg} = \frac{(\dot{E}_D)_{reg}}{T_{ref}} \tag{15}$$

Combustor:

The heat transfer in combustor is:

$$\dot{Q}_{comb} = \dot{m}_B (h_4 - h_3) \tag{16}$$

The exergy destruction of combustor is:

$$(\dot{E}_D)_{comb} = (1 - \frac{T_{ref}}{T_3}) * Q_{comb} + \dot{m}_B(e_3 - e_4) \quad (17)$$

Entropy generation in combustor is:

$$(S_{gen})_{comb} = \frac{(\dot{E}_D)_{comb}}{T_{ref}} \quad (18)$$

Brayton turbine:

Work done by Brayton turbine is:

$$\dot{W}_{T_1} = \dot{m}_B(h_4 - h_5) \quad (19)$$

Exergy destruction of Brayton turbine is:

$$(\dot{E}_D)_{T_1} = \dot{m}_B(e_4 - e_5) - \dot{W}_{T_1} \quad (20)$$

Entropy generation of turbine is:

$$(S_{gen})_{T_1} = \frac{(\dot{E}_D)_{T_1}}{T_{ref}} \quad (21)$$

3.3.4.2 Component equations of Rankine cycle:

Rankine turbine:

The work done by Rankine turbine is:

$$\dot{W}_{T_2} = \dot{m}_R(h_8 - h_9) \quad (22)$$

Exergy destruction in Rankine turbine is:

$$(\dot{E}_D)_{T_2} = \dot{m}_R(e_8 - e_9) - \dot{W}_{T_2} \quad (23)$$

Entropy generation in Rankine turbine:

$$S_{gen} = \frac{(\dot{E}_D)_{T_2}}{T_{ref}} \quad (24)$$

Pump:

Work done by pump is:

$$\dot{W}_P = \dot{m}_R(h_{12} - h_{11}) \quad (25)$$

Exergy destruction in pump:

$$(\dot{E}_D)_P = \dot{W}_P + \dot{m}_R(e_{12} - e_{11}) \quad (26)$$

Entropy generation in pump is:

$$(S_{gen})_P = \frac{(\dot{E}_D)_P}{T_{ref}} \quad (27)$$

Condenser:

Heat rejected by condenser is:

$$\dot{Q}_C = \dot{m}_R(h_{10} - h_{11}) \quad (28)$$

Exergy destruction in condenser is:

$$(\dot{E}_D)_C = \dot{m}_R(e_{10} - e_{11}) + \dot{m}_w(e_{13} - e_{14}) \quad (29)$$

Where $\dot{m}_w$ is the domestic water mass flow rate in Kg/s.

Domestic water mass flow rate:

$$\dot{m}_w = \frac{\dot{Q}_C}{(h_{14} - h_{13})} \quad (30)$$

Entropy generation of condenser is:

$$(S_{gen})_C = \frac{(\dot{E}_D)_C}{T_{ref}} \quad (31)$$

3.4 Waste Heat Recovery Heat Exchanger Analysis method

The rate of heat transfer between streams in the WHRHX is defined as:

$$(\dot{Q}_{WHRHX})_B = \dot{m}_B(h_6 - h_7) \quad \text{for the Brayton stream} \quad (32)$$

$$(\dot{Q}_{WHRHX})_R = \dot{m}_R(h_8 - h_{12}) \quad \text{for the Rankine stream} \quad (33)$$

Where $\dot{m}_B$ and $\dot{m}_R$ are the mass flow rate of the Brayton cycle and Rankine bottoming cycle respectively, 6,7 are the inlet and exit states of WHRHX for Brayton stream and 8,13 are the outlet and inlet states of WHRHX for Rankine cycle respectively.

Exergy destruction in waste heat recovery heat exchanger:

$$(\dot{E}_D)_{WHRHX} = \dot{m}_B(e_6 - e_7) + \dot{m}_R(e_{13} - e_8) \quad (34)$$

The temperature at state 8 is evaluated by:

$$T_8 = T_6 - \Delta T_{hot} \quad (35)$$

The Brayton cycle mass flow rate and ΔT_{hot} are the control parameters. The temperature at state 6 is assumed as 800 K [27].The temperature at state 7 is evaluated by working steam wise starting from condenser. Two methods can be implemented to calculate for two unknowns, mass flow rate of rankine and temperature at state 7.

The method are as follows:

1. Assume a Rankine mass flow rate. Solve for outlet temperature at state 7. Verify that temperature at state 7 is not less than temperature state at 12 as that would not be possible condition. If necessary, modify the Rankine mass flow rate to get valid temperature at state 7.

2. Determine temperature at state 7 by assuming a temperature difference between state 7 and state 12 and then solve for Rankine mass flow rate by Energy balance equation.

In regard to actual system, the bottoming cycle mass flow rate would be independently controlled. Temperature at state 7 and 8 would depend on this Rankine mass flow rate and heat transfer properties of WHRHX. By assuming that, the heat transfer properties of WHRHX are such that the prescribed temperature difference occurs, a numerical heat transfer analysis of WHRHX is avoided. So, first method is used in the EES analysis. The temperature at exit of WHRHX for Brayton cycle is evaluated as:

$$T_7 = T_{12} + \Delta T_{cold} \tag{36}$$

Where ΔT_{cold} is temperature difference of the cold side of WHRHX.

3.5 Economic Analysis of System

The evaluation of the total capital cost of the cycle system [28] is determined from the sum of the cost of each component which is discussed below:

The cost of waste heat recovery heat exchanger is calculated by:

$$C_{WHRHX} = \frac{527.7}{397} * (B_{1,WHRHX} + B_{2,WHRHX} * F_{M,WHRHX} * F_{P,WHRHX}) F_S * C^0_{WHRHX} \tag{37}$$

Where $B_{1,WHRHE}$ and $B_{2,WHRHE}$ are constant for waste heat recovery heat exchanger type, $F_{M,WHRHX}$ are material factor , $F_{P,WHRHX}$ is the pressure factor, F_S is the additional factor of waste heat recovery heat exchanger.

C^0_{WHRHX} is the basic cost of waste heat recovery heat exchanger operating at ambient condition.

The basic cost of waste heat recovery heat exchanger is:

$$C^0_{WHRHX} = K_{1,WHRHX} + K_{2,WHRHX} * \log(A_{WHRHX}) + K_{3,WHRHX} * \log(A_{WHRHX})^2 \tag{38}$$

Where $K_{1,WHRHX}$, $K_{2,WHRHX}$ and $K_{3,WHRHX}$ are the constant of waste heat recovery types and A_{WHRHX} is the area of waste heat recovery heat exchanger.

Now, area of waste heat recovery heat exchanger is calculated by:

$$A_{WHRHX} = \frac{\dot{Q}_{WHRHX}}{(U * \Delta T_m)} \tag{39}$$

Where U is the overall heat transfer coefficient and ΔT_m is the logarithm mean temperature difference.

Overall heat transfer coefficient is:

$$U = \frac{1}{(\frac{1}{h_f} + \frac{1}{h_{wall}})} \tag{40}$$

Where h_f is the heat transfer coefficient of working substance i.e. CO_2 and h_{wall} is heat transfer coefficient of shell tube waste heat recovery heat exchanger.

The logarithm mean temperature difference is :

$$\Delta T_m = \frac{(T_6 - T_8) - (T_7 - T_{12})}{\ln((T_6 - T_8)/(T_7 - T_{12}))} \tag{41}$$

The cost of turbine is given by:

$$C_{tur} = \frac{527.7}{397} * F_{MP,tur} * F_S * C^0_{tur} \tag{42}$$

Where $F_{MP,tur}$ is the material and pressure factor of turbine and C^0_{tur} is the basic cost of turbine.

The basic cost of turbine is :

$$\log(C^0_{tur}) = K_{1,tur} + K_{2,tur} * \log(W_{T,2}) + K_{3,tur} * \log(W_{T,2})^2 \tag{43}$$

Where $K_{1,tur}$, $K_{2,tur}$ and $K_{3,tur}$ are the constant of turbine and $W_{T,2}$ is the Rankine turbine work.

The cost of pump can be evaluated by:

$$C_{Pump} = (B_{1,P} + B_{2,P} * F_{M,P} * F_{P,P}) F_S * C^0_{Pump} \tag{44}$$

Where $B_{1,P}$ and $B_{2,P}$ are constants for pump type, $F_{M,P}$ is the material factor and $F_{P,P}$ is the pressure factor and C^0_{Pump} is the basic cost of pump.

The basic cost of pump is:

$$\log(C^0_{Pump}) = K_{1,P} + K_{2,P} * \log(W_{Pump}) + K_{3,P} * \log(W_{Pump})^2 \quad (45)$$

Where $K_{1,P}$, $K_{2,P}$ and $K_{3,P}$ are constant for pump type and W_{Pump} is the Rankine Pump work.

The total cost of system is calculated by:

$$C_{total} = C_{WHRHX} + C_{tur} + C_{Pump} \quad (46)$$

Chapter 4

4. RESULTS AND DISCUSSION

The objective of this study is to determine the best possible solution for the problem of recovering as much energy from the exhaust waste heat stream from naval ships gas turbine exhaust using transcritical CO_2 cycle. In below paragraph we evaluate the results of a parametric study for the transcritical CO_2 cycle using previously described model. The transcritical CO_2 cycle is heated by the waste heat coming from the exhaust of naval ships gas turbine exhaust. The initial parameter used to evaluate the transcritical CO_2 cycle which is explain in table 3.2.

4.1 Parametric Analysis

The first step of the analysis is the single variable of each parameter in table 3.2. In section 3.3, we discussed each parameters in detail of the procedure for the analysis. The mass flow rate of topping cycle is remain constant at 1 kg/s, unless until specified.

4.1.1 Variation of Turbine Inlet Temperature

The turbine inlet temperature varied from 1200K-1500K. Figure 4.1 shows the energetic efficiency and exergetic efficiency of Brayton cycle verses turbine inlet temperature. In Figure 4.1, also shows the combustion efficiency. Plot shows when the turbine inlet temperature increases, all the efficiency increases either energetic or exergetic.
Figure 4.2 shows the energetic efficiency of Brayton cycle, combined cycle and exergetic efficiency of combustor verses turbine inlet temperature. This plot also indicates with increase in turbine inlet temperature all energetic efficiency are increases and exergetic efficiency of combustor also increases.

TIT(K)	Brayton cycle Efficiency	Second law Eff. Of Combined cycle	Second law efficiency of combustor	First law Combined cycle Eff.
1200	0.2225	0.2147	0.7888	0.5197
1250	0.2521	0.2406	0.8036	0.538
1300	0.2789	0.2646	0.8173	0.5545
1350	0.3032	0.2872	0.8300	0.5696
1400	0.3254	0.3082	0.8417	0.5833
1450	0.3457	0.3279	0.8527	0.5958
1500	0.3643	0.3465	0.863	0.6073

Table 4.1: Results of parametric study due to TIT

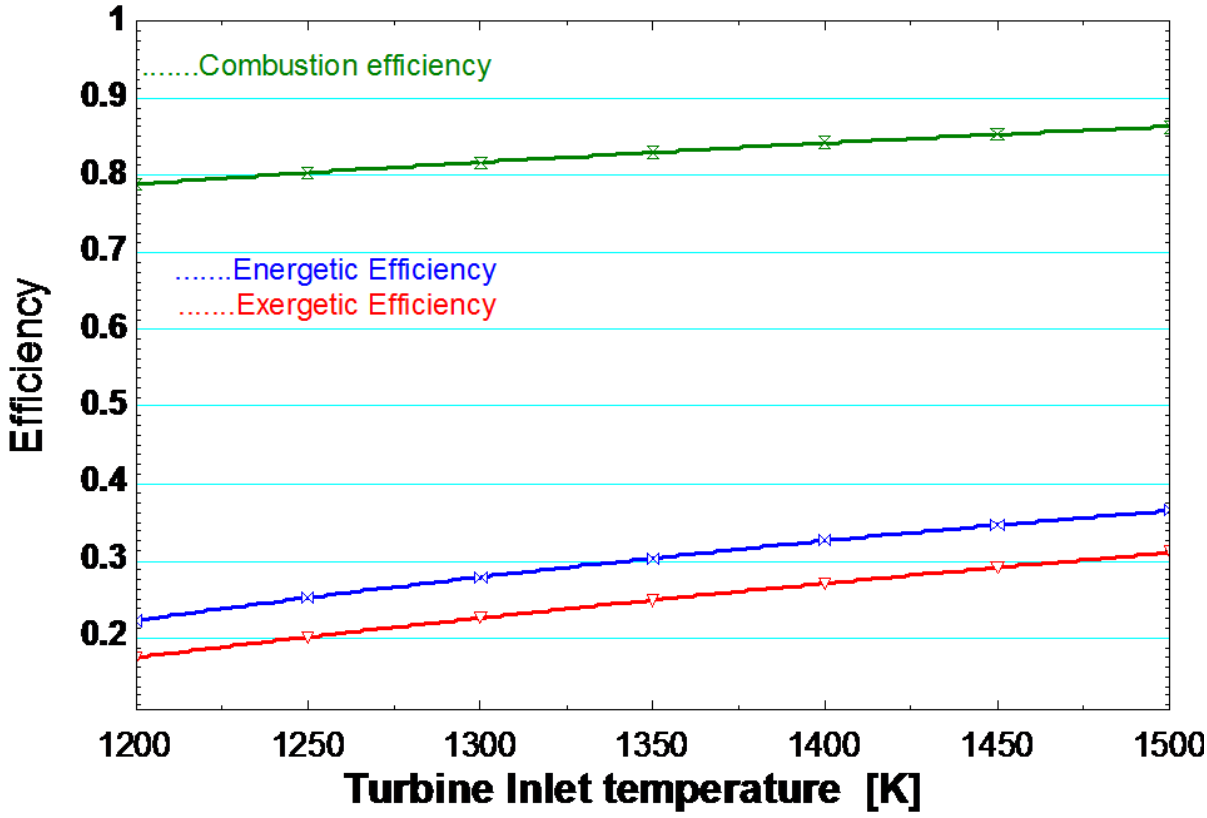

Figure 4.1: Efficiency vs Turbine Inlet Temperature

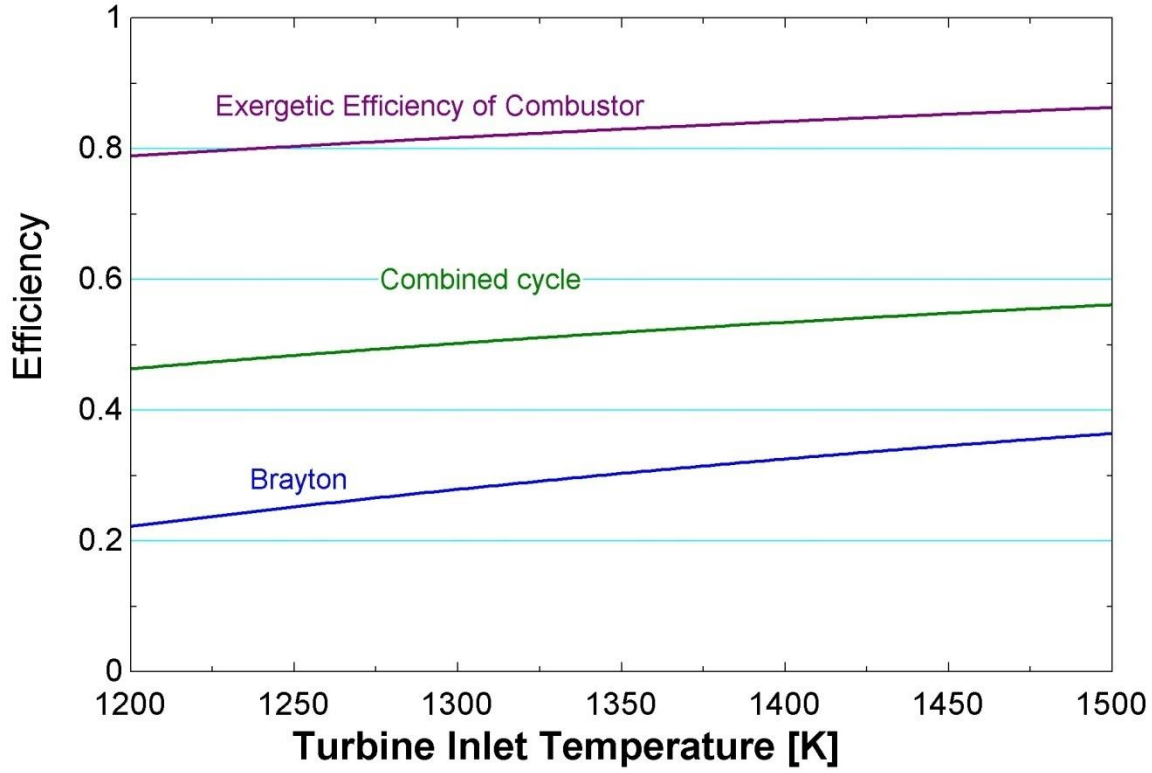

Figure 4.2: Efficiency vs Turbine Inlet Temperature

The second law efficiency of Combustor is surprisingly increasing with the increase in turbine inlet temperature. This surprising results happens because of recuperature. The increase in high temperature exit from the turbine increases the combustor inlet temperature, so the exergetic efficiency of combustor increases.

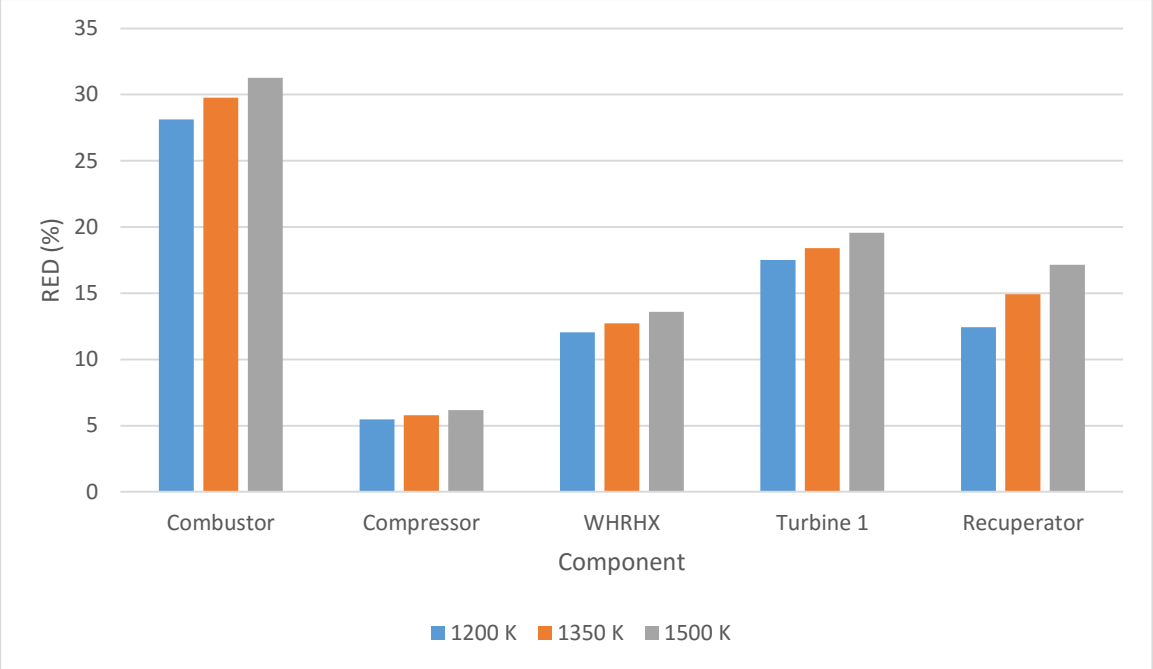

Figure 4.3: Turbine Inlet Temperature vs RED of Different component

Figure 4.3 shows the variation of Relative exergy destruction of component wise verses turbine inlet temperature. Combustor has the largest contribution in exergy destruction whereas compressor has the smallest contribution in exergy destruction.

4.1.2 Variation of Ambient Temperature

The ambient temperature is varied from 278 K to 300 K. The maximum limiting temperature of 300 K is allow for a 2 K temperature difference between the critical temperature of CO_2 and cooling water in condenser. The bottoming CO_2 cycle becomes entirely supercritical at a temperature above 302 K leaving the condenser.

Figure 4.4 shows the variation of ambient temperature verses system power output, system first and second law efficiency. It can be seen from the figure that the system power output and system first and second law efficiency all decreases with increase of ambient temperature. However, like mass flow rate of air ambient temperature can not be adjusted. The system output net power will greatly decrease in summer (ambient temperature is about 35^{o}C i.e. 308 K) as compared to winter (ambient temperature is about 5^{o}C i.e. 278 K), to less than the nominal value by more than 30 %.

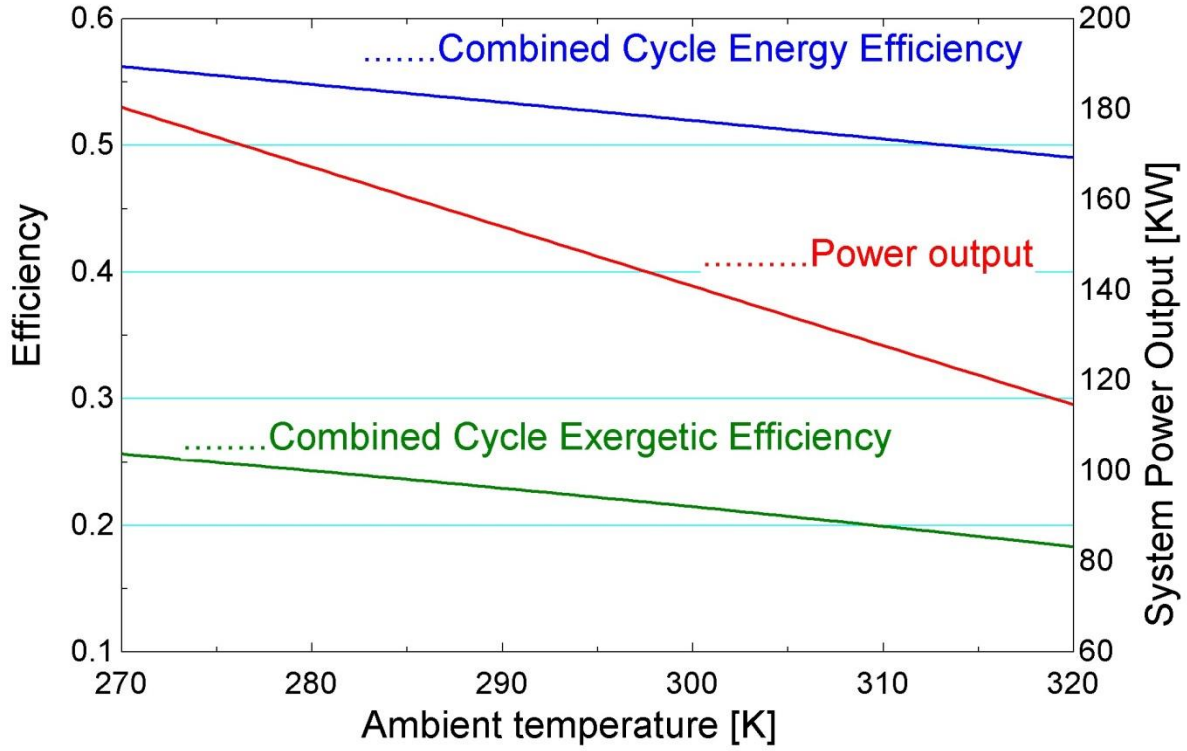

Figure 4.4: Ambient temperature verses Power Output/Efficiency

4.1.3 Variation of Brayton cycle Pressure Ratio

The topping cycle pressure ratio is varied from 3 to 19. Here inlet temperature of turbine is present at 1350 K. Figure 17 shows variation of Brayton cycle pressure ratio verses net specific work output and efficiency of Brayton cycle.

From figure 4.5, it is observedthat for maximum net specific work, first law efficiency of Brayton cycle and system second law efficiency simultaneously, there does not exist a single pressure ratio. The maximum efficiency is 33 % which occurs at pressure ratio of 4.5 whereas the maximum net specific output is 142 KJ/Kg which occurs at a pressure ratio of 8.5 and maximum second law efficiency of 28.53 % at pressure ratio of 6.

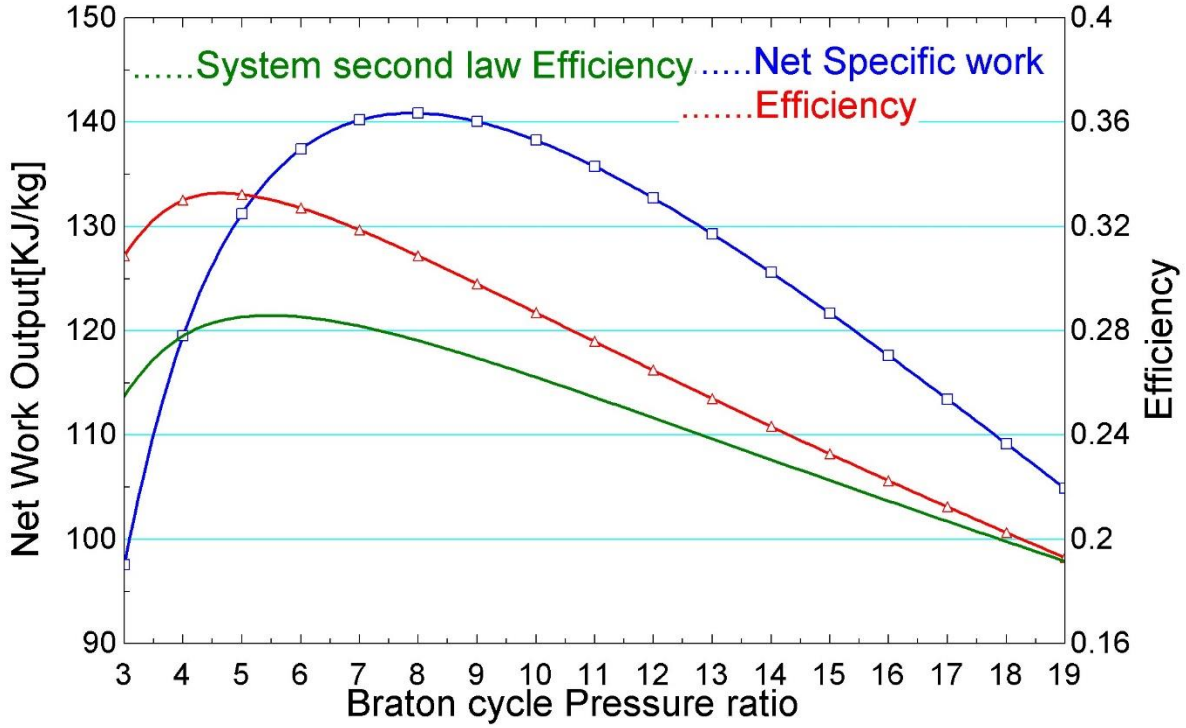

Figure 4.5: Brayton cycle Net Specific WOrk/Efficiency verses Brayton cycle Pressure Ratio

Figure 4.6 shows the variation of net specific work with the Brayton cycle pressure ratio and turbine inlet temperature. Figure shows with the decrease in the turbine inlet temperature, the pressure ratio at which maximum net specific work occurs is decreases.

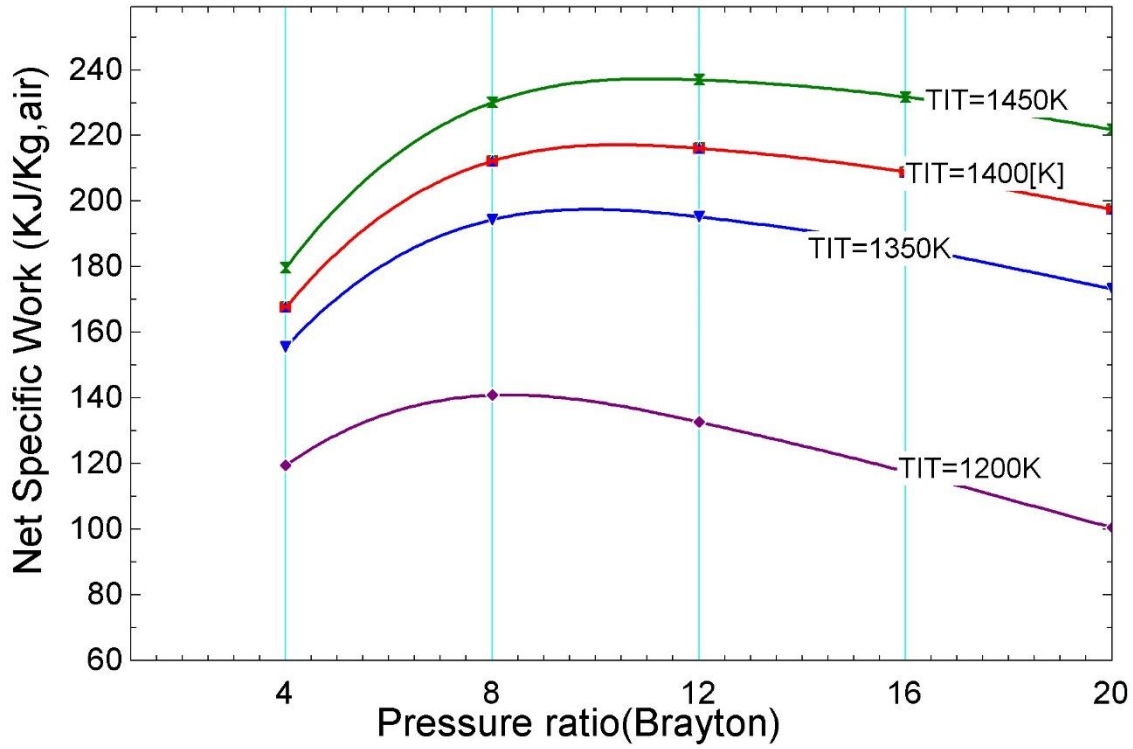

Figure 4.6: Effect of Pressure ratio and TIT on the net specific work

4.1.4 Variation of Compressor/Turbine Isentropic Efficiency

For the parametric study of the compressor and turbine efficiency, both the values will set nearly equal to each other and varied simultaneously. The most relevant data is given in table 4.2.An interesting observation is with increase in compressor isentropic efficiency, the heat required for combustion is increases because the temperature at exit of compressor is decreases. Due to this lower temperature exit from compressor, the exit of the recuperator is also lower. So more heat is required for combustion occurs. It decreases the heat supplied to Brayton cycle. So the system efficiency is increases.

At various turbine isentropic efficiency, table 4.3 shows the variation of turbine outlet temperature for Brayton cycle, heat of combustion, total exergy destruction, recuperator heat transfer and system efficiency.

Compressor efficiency	Combined cycle efficiency	Combustor heat transfer (KW)	Total exergy Destruction (KW)	Recuperator heat transfer (KW)
0.8	0.462	521.1	323.1	3.084
0.85	0.4927	525.1	326.3	25.75
0.9	0.5197	528.7	328.6	45.9
0.95	0.5435	531.9	330.1	63.93
1	0.5647	534.7	330.9	80.15

Table 4.2: Results of parametric study due to compressor efficiency

Turbine Efficiency	Combined cycle efficiency	Combustion heat transfer (KW)	Total exergy destruction (KW)	Recuperator Heat transfer (KW)	Turbine 1 exit temperature(K)
0.7	0.2463	550.9	315.3	201.4	906.3
0.75	0.2963	582.2	313.4	170.1	873.4
0.8	0.3412	613.5	311.2	138.8	840.3
0.85	0.3817	644.8	308.8	107.5	806.9
0.9	0.4185	676.1	306.1	76.2	773.3
0.95	0.452	707.4	303.1	44.91	739.5
1	0.4827	738.7	299.7	13.62	705.4

Table 4.3: Results of parametric study due to turbine efficiency

Due to increase in turbine isentropic efficiency, turbine exit temperature decreases and system efficiency increases. A reduction in the turbine outlet temperature reduces the recuperator heat transfer which consequently reduces the turbine inlet temperature. This requires more heat for combustion. That's why system efficiency increases.

4.1.5 Variation of Recuperator Effectiveness

Range of recuperator effectiveness is varied from 60% to 100%. Figure 4.8 shows the variation of recuperator heat transfer and Topping cycle energetic efficiency and system exergetic efficiency verses recuperator effectiveness. Plot shows with increase of recuperator effectiveness, the recuperator heat transfer, Brayton cycle efficiency any system second law efficiency all increases. As a result less heat will transfer in combustion. The maximum value of energetic efficiency of Brayton cycle is 22.5% at perfect recuperator effectiveness by maintaining power output while decreasing fuel utilisation.

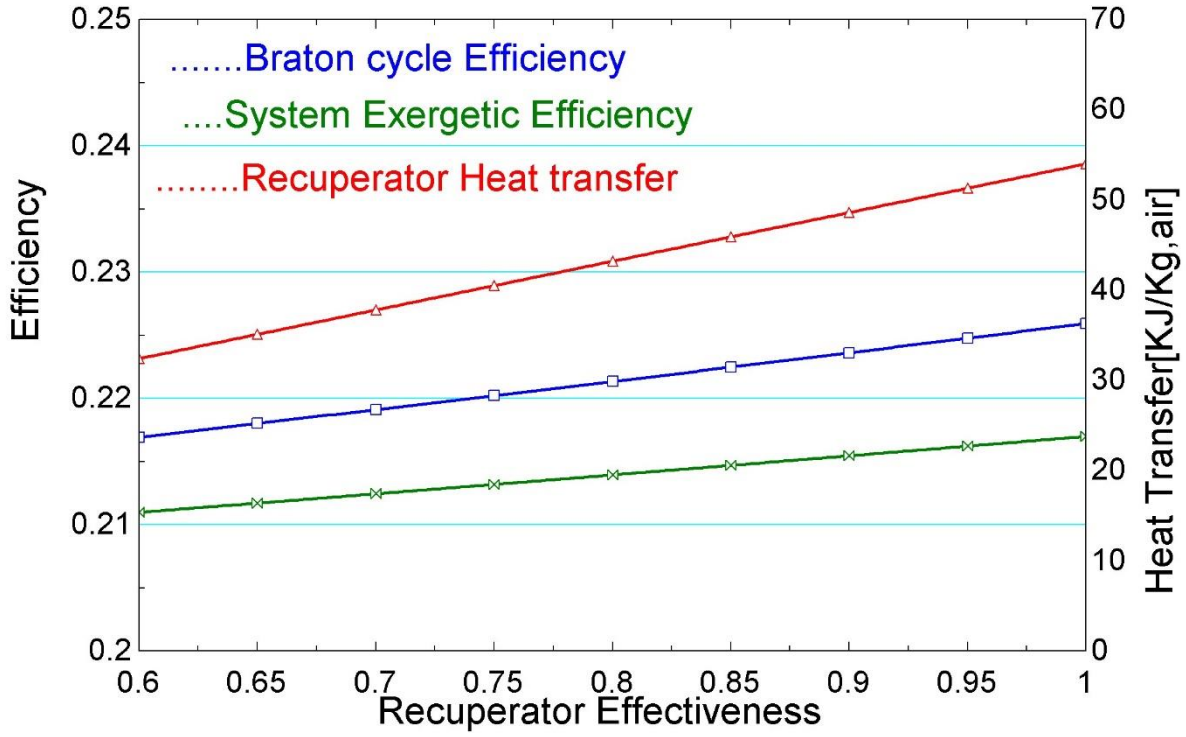

Figure 4.7: Efficiency/Heat transfer verses Recuperator effectiveness

Figure 4.8 shows the variation of combustion inlet temperature and regenerator heat transfer verses recuperator effectiveness. Plot shows with increase of recuperate reffectivess, inlet temperature of combustion increases and amount heat transfer for combustion is decreases.

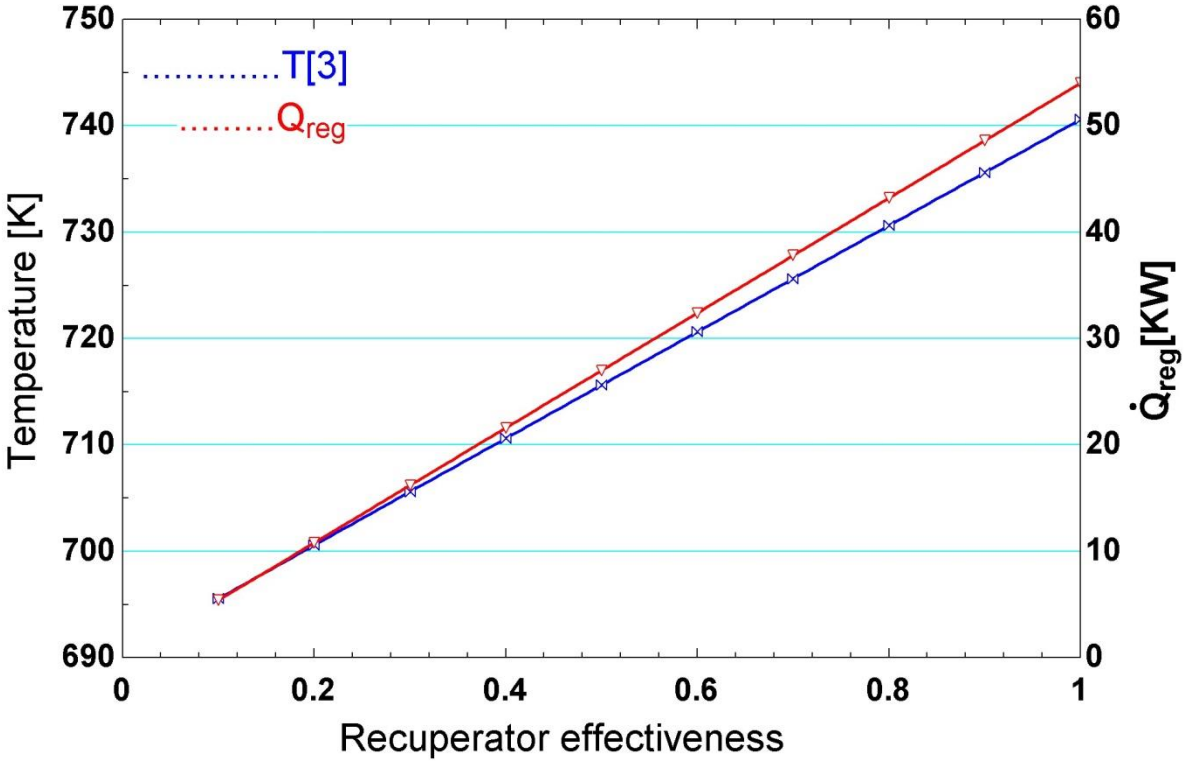

Figure 4.8: Combustion inlet temperature/Heat transfer verses recuperator effectiveness

4.1.6 Variation of Rankine Cycle Maximum Pressure

The range of maximum pressure in the Rankine cycle will be varied from 10000 KPa to 20000 KPa. The minimum pressure of Rankine cycle will be evaluated from temperature of saturated state CO_2 leaving the condenser. The exergy destruction of the component of Rankine cycle for three different maximum pressure is plotted in figure 4.9. It is shown from the figure that exergy destruction for pump and condenser are relatively small. Due to increase in maximum cycle pressure of Rankine cycle, exergy destruction of WHRHX, turbine 2 and pump increases. Because an expansion device becomes less efficient at higher pressure that's why exergy destruction of turbine 2 increases.

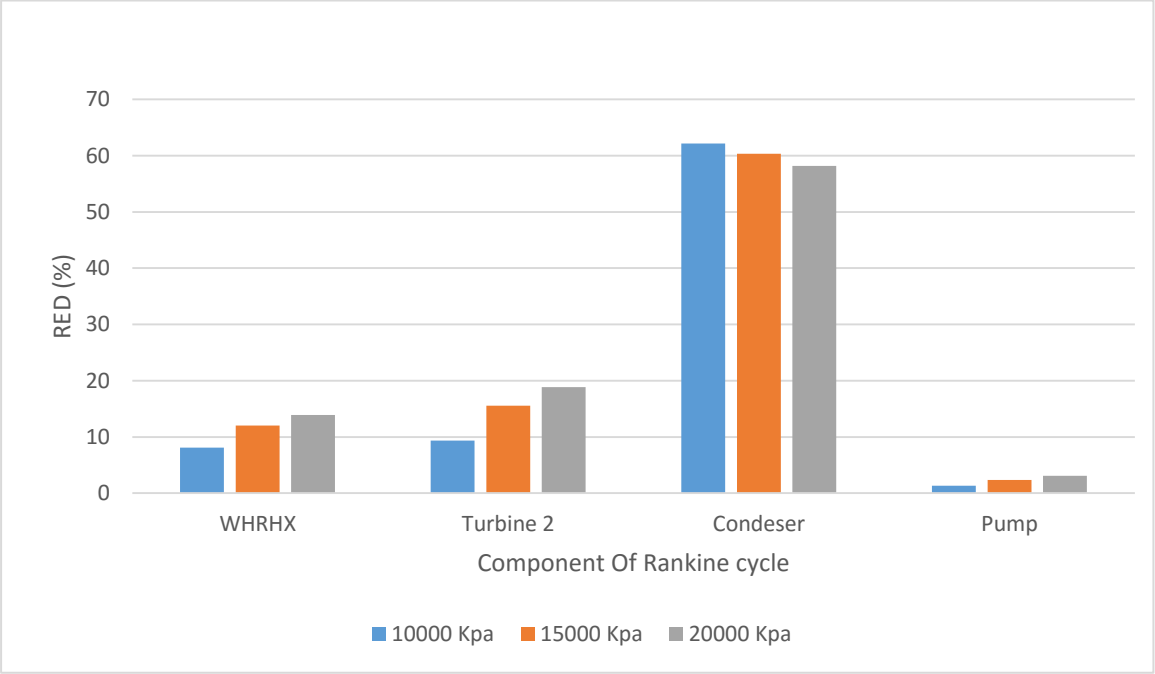

Figure 4.9: Relative Exergy Destruction verses Bottoming cycle maximum Pressure

4.1.7 Variation of Exhaust Temperature from Naval Ship Gas Turbine

The exhaust temperature from naval ships gas turbine is varied from 733K to 900K [27]. For analysis in this work, it is taken as 800 K. Figure 4.10 shows the variation of System power output and system efficiency verses naval ships gas turbine exhaust temperature. Plot shows that with the increase in exhaust temperature, both system power output and system efficiency increases. The maximum value of system power output is 145 KW at 900 K exhaust temperature. Also the maximum value of system efficiency is 57 % at 900 K exhaust temperature.

Figure 4.11 shows the variation of relative exergy destruction of each component of Rankine cycle verses exhaust temperature from naval ships gas turbine exhaust. Plot shows the relative exergy destruction of turbine 2 and WHRHX are greatly effected gas turbine exhaust temperature. With the increase of exhaust temperature, exergy destruction of turbine 2 is increases because large amount of heat is transferred into Rankine cycle.

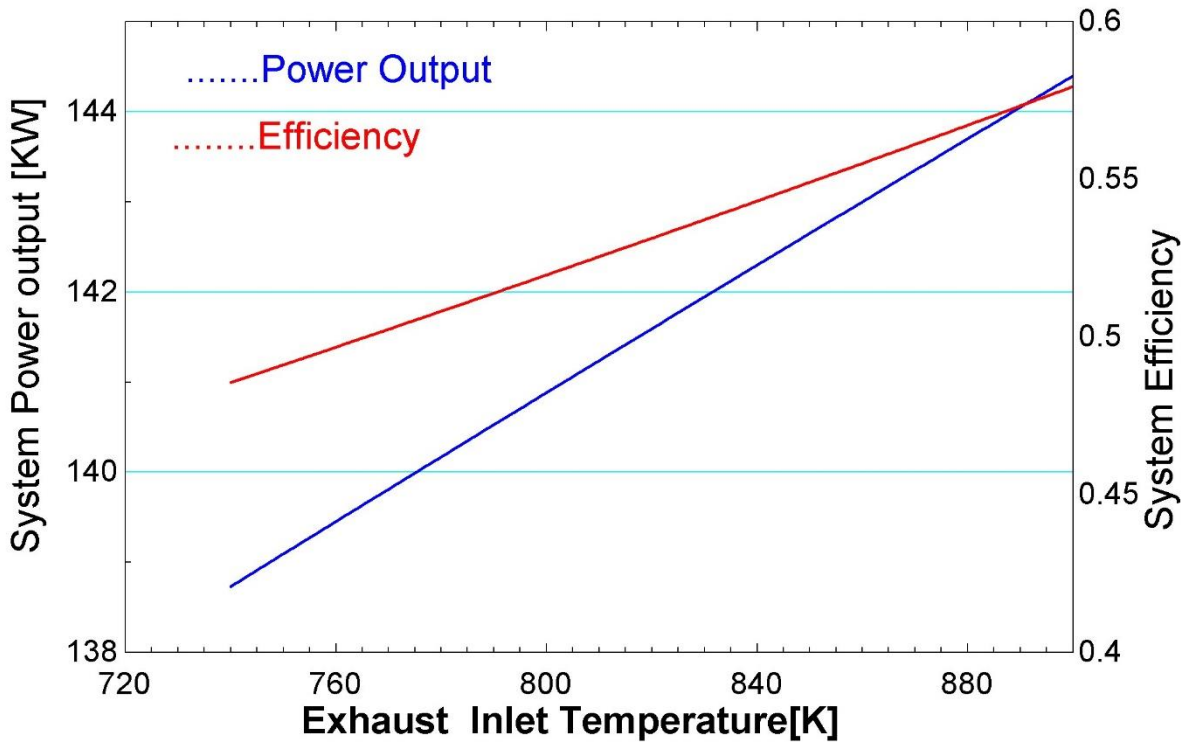

Figure 4.10: System Power Output/System Efficiency verses Gas turbine Exhaust Temperature

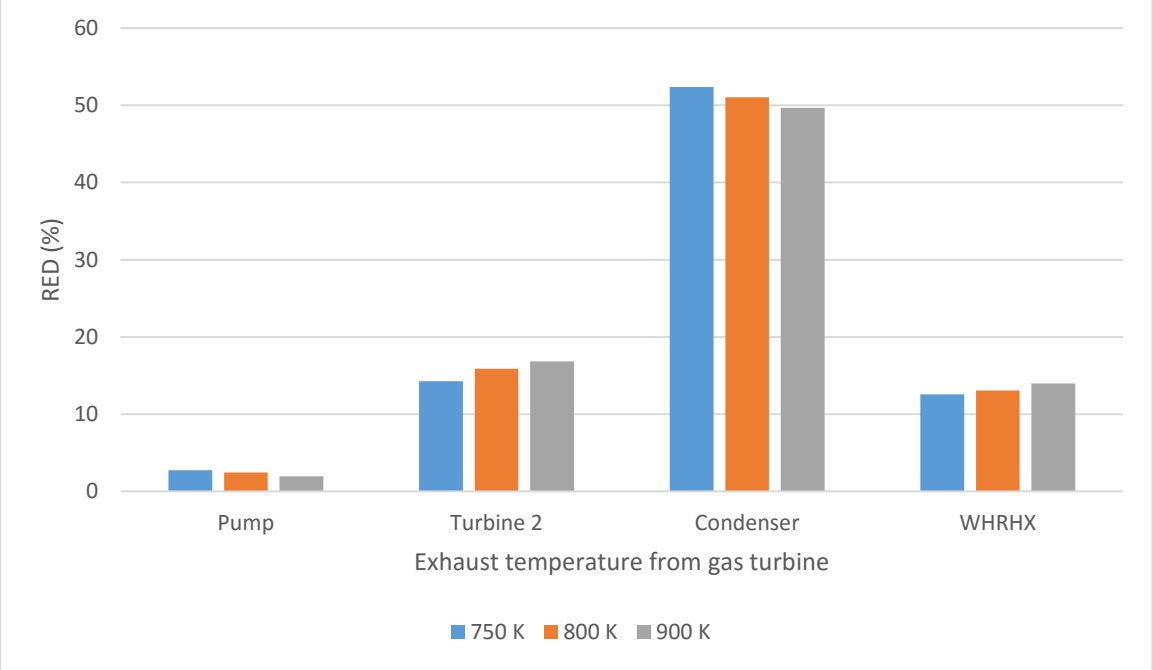

Figure 4.11: Relative Exergy Destruction of Rankine cycle component verses Gas turbine exhaust temperature

4.1.8 Variation of WHRHX Temperature Difference

The hot side temperature difference of WHRHX is varied from 12K to 40 K. Table 4.4 shows the variation of hot side temperature difference of WHRHX. With the increase of temperature difference, the WHRHX heat transfer decreases which results in lower turbine work and exergy destruction in the WHRHX also decreases but the exergetic efficiency of WHRHX increases. The less expected results comes in the condenser. The temperature difference in the condenser reduces because of lower turbine exit temperature, thus increases the condenser exergetic efficiency and reduces the condenser exergy destruction. Due to decrease in the heat transfer rate in WHRHX, the flow rate of domestic hot water is decreases.

dT_{HOT} (K)	WHRHX heat transfer (KW)	Rankine cycle Eff.	System power output (KW)	WHRHX exergetic efficiency	Combined cycle first law efficiency	WHRHX exergy destruction (KW)	Combined cycle second law efficiency
12	60.88	0.3098	140.9	0.8771	0.4633	39.59	0.231
20	58.92	0.3243	141.2	0.9051	0.4746	39.31	0.2315
30	56.46	0.3437	141.5	0.9416	0.4897	38.96	0.2322
40	54	0.3648	141.9	0.9798	0.5061	38.62	0.2329

Table 4.4: Variation of WHRHX hot side temperature difference

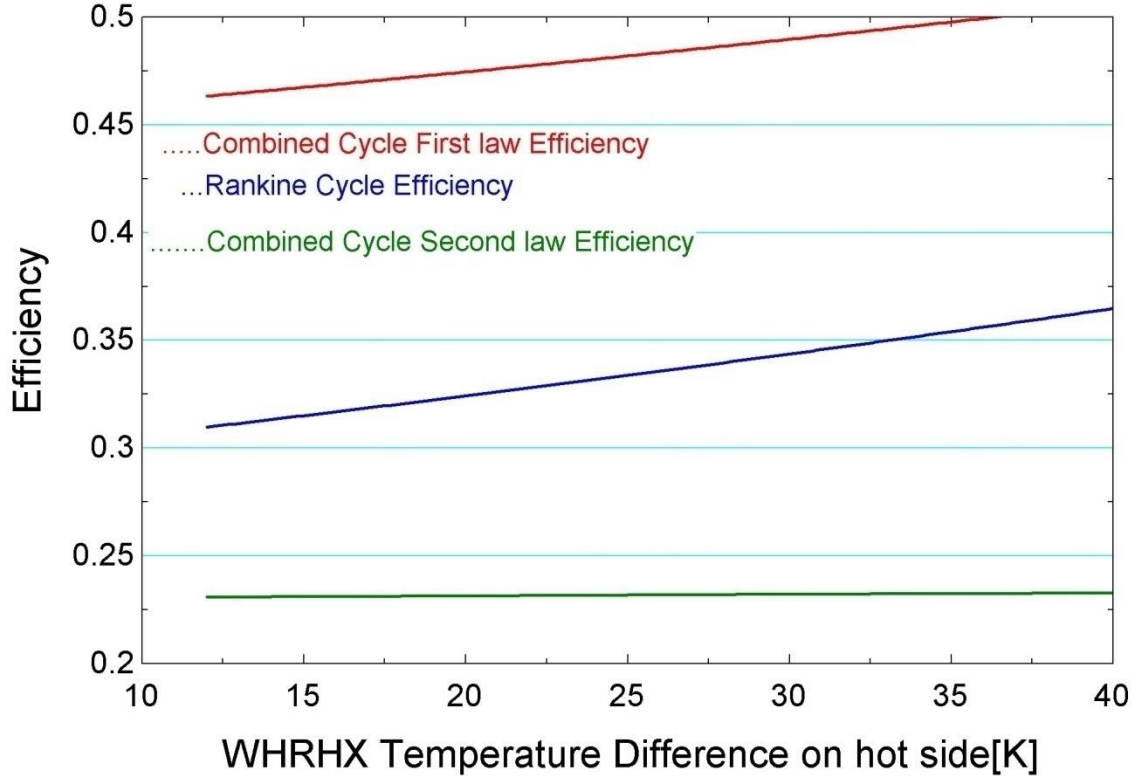

Figure 4.12: Efficiency verses WHRHX hot side temperature difference

Figure 4.12 shows the variation of Rankine cycle first law efficiency, combined cycle first law efficiency and combined cycle second law efficiency with the variation of waste heat recovery heat exchanger hot side temperature difference. Figure shows with increase in hot side temperature difference of waste heat recovery heat exchanger, all the three efficiency i.e. Rankine cycle first law efficiency, combined cycle first law efficiency and combined cycle second law efficiency increases. The maximum value of Rankine cycle efficiency is 36.48 % at temperature difference of 40 K. The maximum value of combined cycle first law efficiency is 50.61% at temperature difference of 40 K. The maximum value of combined cycle second law efficiency is 23.29 % at temperature difference of 40 K.

4.1.9 Variation of mass flow rate

The Rankine mass flow rate is varied from 0.1 Kg/s to 1Kg/s. Here for analysis it is taken as 0.2 Kg/s. Figure 4.13 shows System power output and Rankine Power output increases with the increase in mass flow rate of Rankine cycle. The maximum value of power output for Rankine cycle is 120 KW at 1 Kg/s and maximum value of system output is 235 KW at 1 Kg/s.

Figure 4.14 shows the variation of combined cycle power output and Brayton cycle power output verses Brayton mass flow rate. Both power increases with the increase in mass flow rate of Brayton.

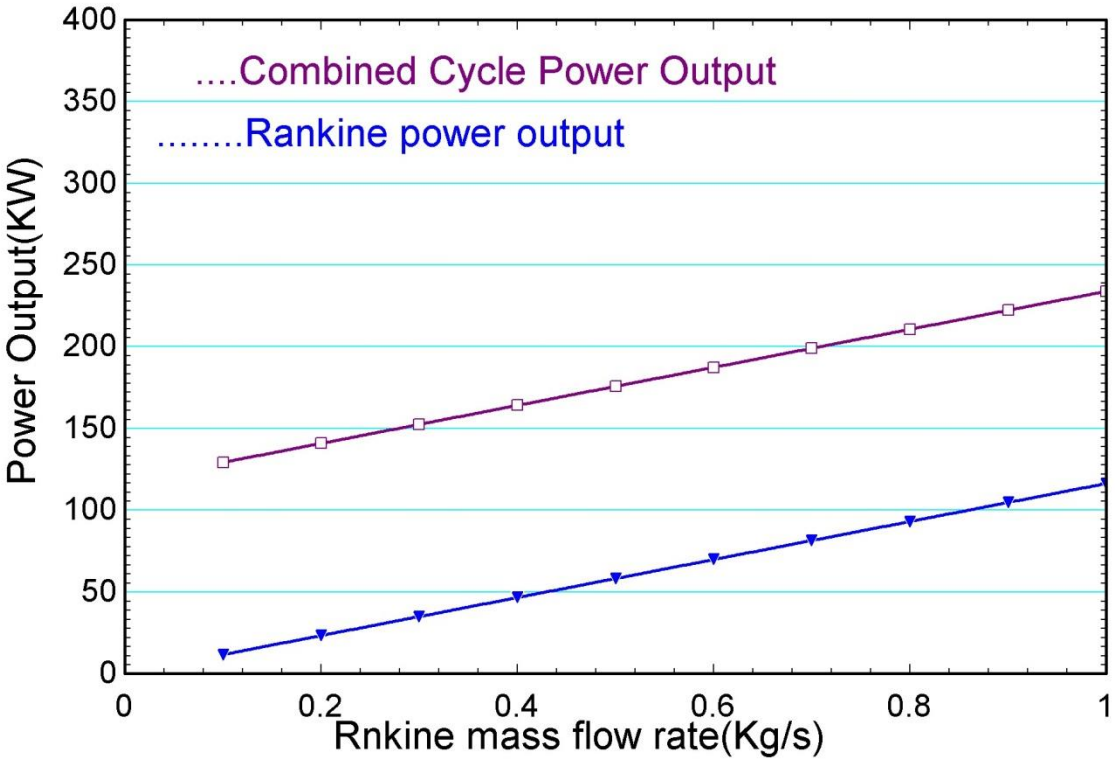

Figure 4.13: Power output verses Rankine mass flow rate

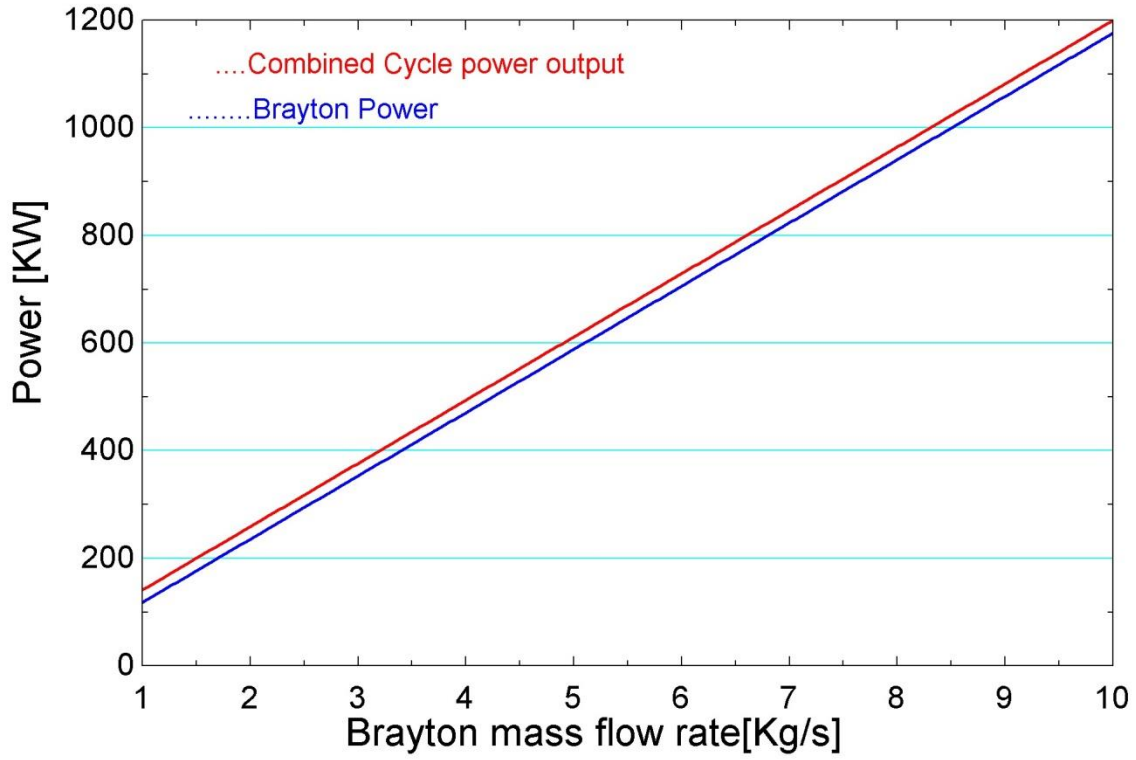

Figure 4.14: Power output verses Brayton mass flow rate

4.2 Relative Pressure Loss

A relative pressure loss is used in analysis. The amount of internal irreversibility may be shown by "pressure loss". So A relative pressure loss is given by:

$$P_e = (1 - \Delta P) * P_i \tag{47}$$

Where P_e is the outlet pressure and P_i is the inlet pressure.

Entropy change by a process may be written as

$$dS = dS_e + dS_i \tag{48}$$

Where dS_e is the entropy change due to external effects and dS_i is the entropy change due to internal effects. A zero pressure loss shows a process with no internal irreversibility and does no entropy change by internal effects. In this case, total entropy change is the entropy change due to heat transfer. The analysis is done at relative pressure losses of 0%, 3% and 5%. To avoid interaction between components, one component is analysed at a time with all other pressure loss assume to be zero. Table 4.5 shows the variation of component relative pressure loss with the component exergy destruction and component exergetic efficiency. From Eq. 15, with increase in relative pressure loss exergy destruction increases. The condenser is least effected by relative pressure loss with 0.2779 KW of exergy destruction at 5 % pressure loss. The combustor is most effected with 95.68 KW of exergy destruction at 5% pressure loss.

Component	Relative pressure loss	Component exergy destruction (KW)	Component exergetic efficiency
Regenerator	0.0%	67.43	40.28%
	3%	61.41	51.85%
	5%	57.28	62.93%
Combustor	0.0%	92.92	79.73%
	3%	94.56	79.23%
	5%	95.68	78.88%
Waste heat recovery heat exchanger	0.0%	42.31	84.14%
	3%	40.70	86.18%
	5%	39.59	87.71%
Condenser	0.0%	———	———
	3%	0.632	21%
	5%	0.2779	4.41%

Table 4.5: Variation of relative pressure loss

A pressure loss in one component also affects the other component within the cycle. Figure 4.15 shows the variation of relative exergy destruction of each component in system verses three relative pressure loss of recuperator. With increase in recuperator relative pressure loss, relative exergy destruction of recuperator and turbine 1 decreases.

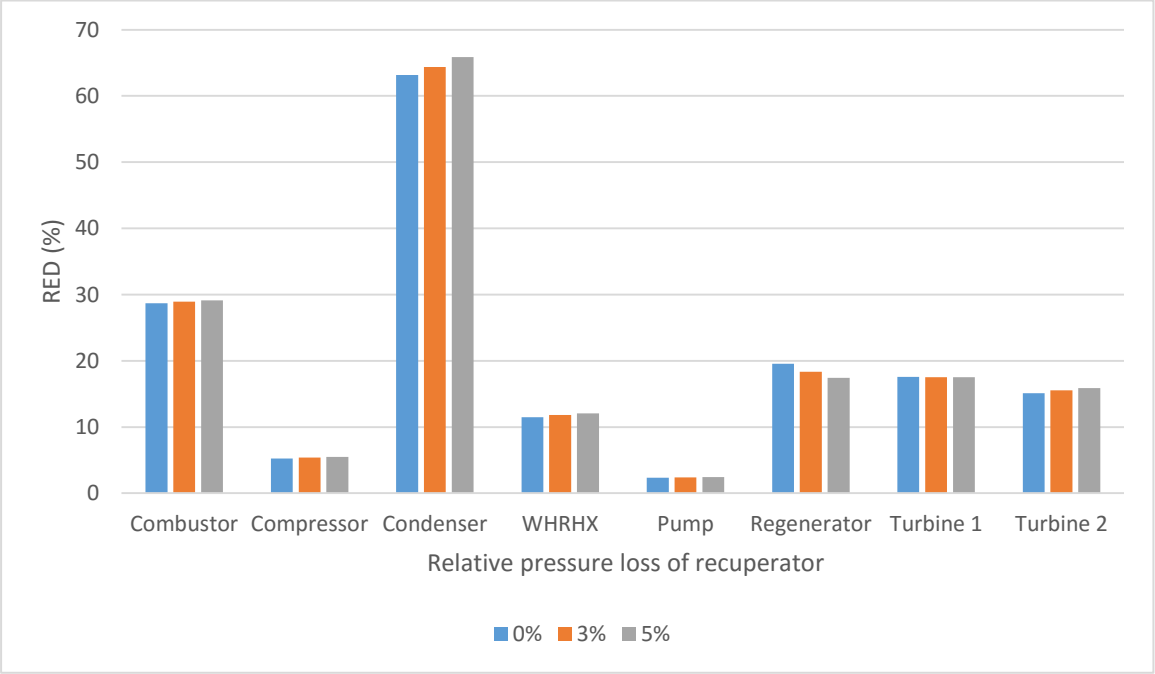

Figure 4.15: Relative exergy destruction for three pressure loss of recuperator

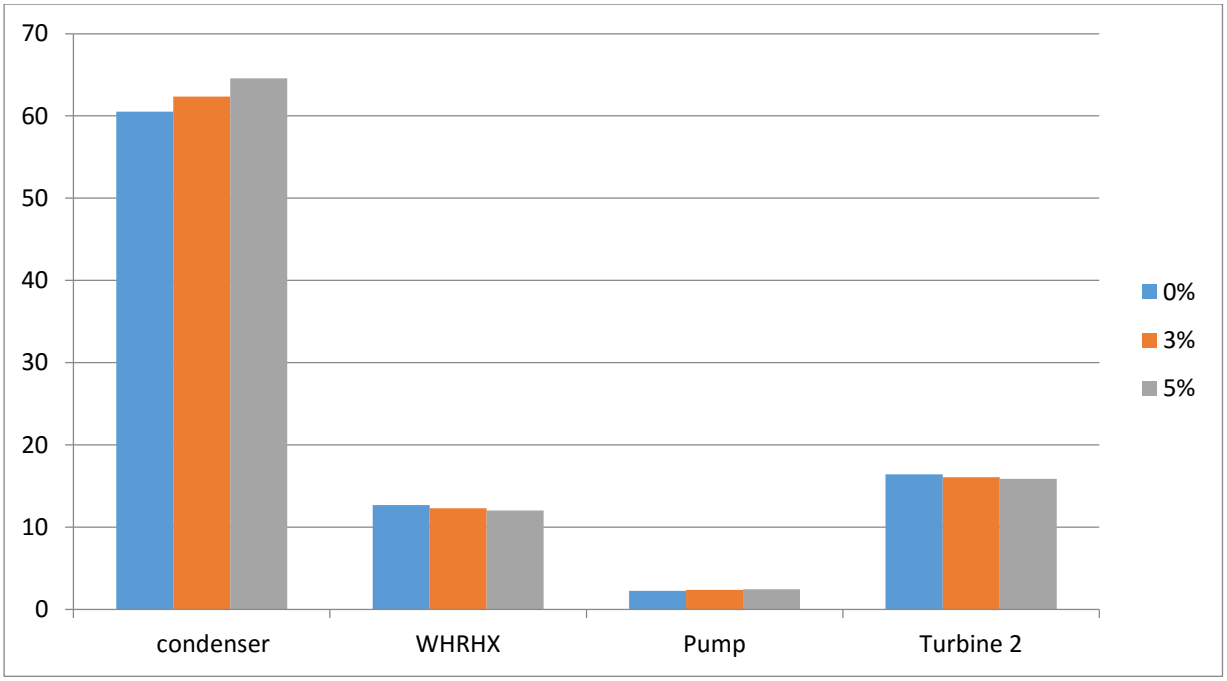

Figure 4.16: Relative exergy destruction for three pressure loss of WHRHX

There is negligible effect in condenser of relative pressure loss because the constant temperature of combustor outlet (1350 K) reduces the impact of pressure loss on the stream's high exit enthalpy.

Figure 4.16 shows the variation of relative exergy destruction of each component of Rankine cycle verses three relative pressure loss of waste heat recovery heat exchanger. With increase of relative pressure loss in the WHRHX, the relative exergy destruction of WHRHX and turbine 2 decreases. But there is negligible increase of relative exergy destruction in case of condenser because expansion ratio in the Rankine cycle decreases which results in higher turbine outlet temperature. The Brayton side WHRHX exit is discharged into environment. So a higher upstream pressure or "back pressure" occurs to counteract a pressure loss in WHRHX. This back pressure in the Brayton cycle slightly reduces the expansion ratio in the Brayton cycle. So, accordingly a slight reduction in Brayton work is observed.

4.3 Economic Analysis of system

This section demonstrate the effects of Rankine turbine inlet pressure and Rankine turbine outlet pressure on total cost of system. Figure 4.17 shows the variation of total cost of system with the maximum Rankine pressure and exhaust temperature from naval ships gas turbine. With increase in the maximum Rankine pressure, total cost is increases and it is also increase with increase in exhaust temperature.

Figure 4.18 shows the variation of total cost of the system with the minimum Rankine pressure and exhaust temperature from naval ships gas turbine. With increase in minimum Rankine cycle pressure, total cost is increase and it also increases with increase in exhaust temperature.

Figure 4.19 shows the variation of total cost of system with the exhaust temperature from naval ships gas turbine. Figure shows with increase in temperature from naval ships gas turbine exhaust, the total cost of the system is increases.

Figure 4.20 shows the variation of total cost of the system with the Rankine cycle mass flow rate. Figure shows with increase in the mass flow rate of Rankine cycle, total cost of the system increases.

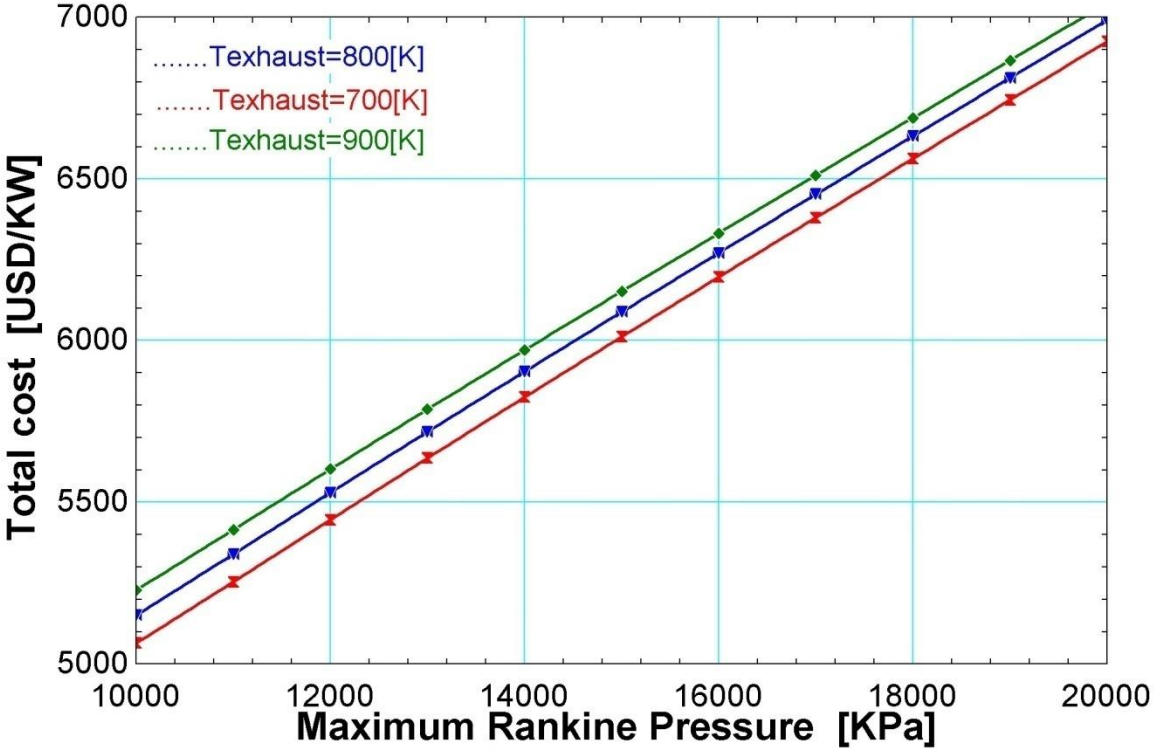

Figure 4.17: Maximum Rankine Pressure verses Total cost

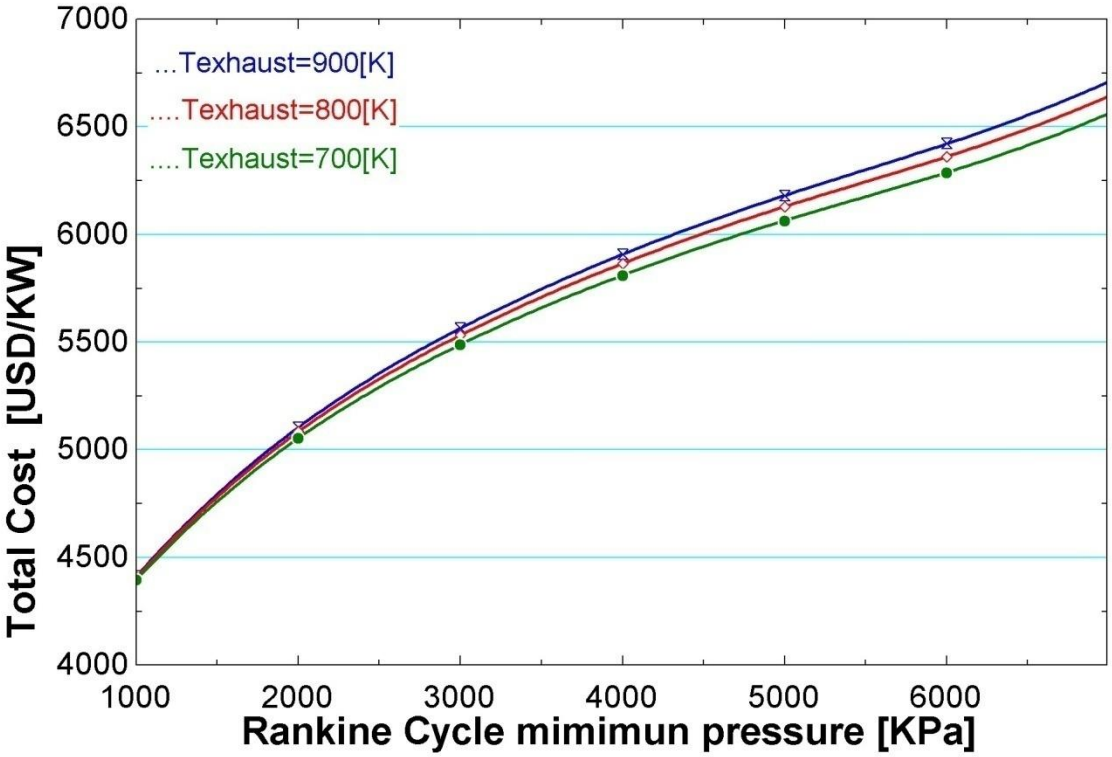

Figure 4.18: Minimum Rankine Pressure verses Total Cost

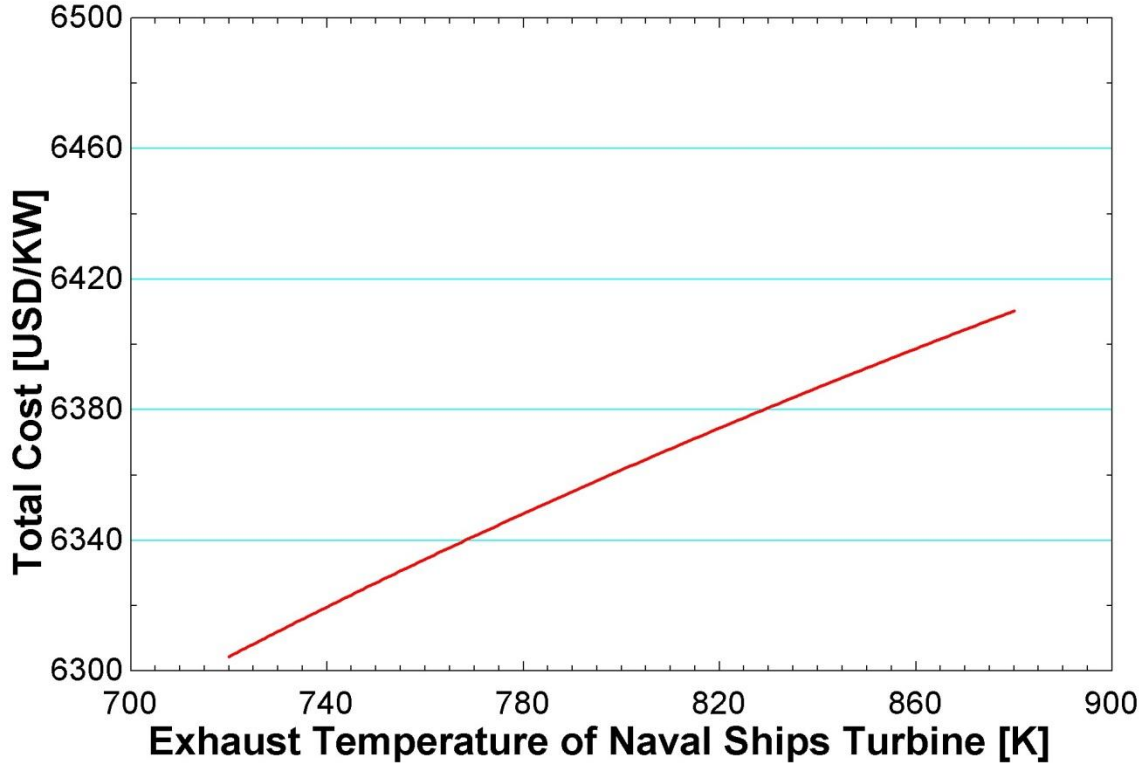

Figure 4.19: Total Cost verses Exhaust Temperature

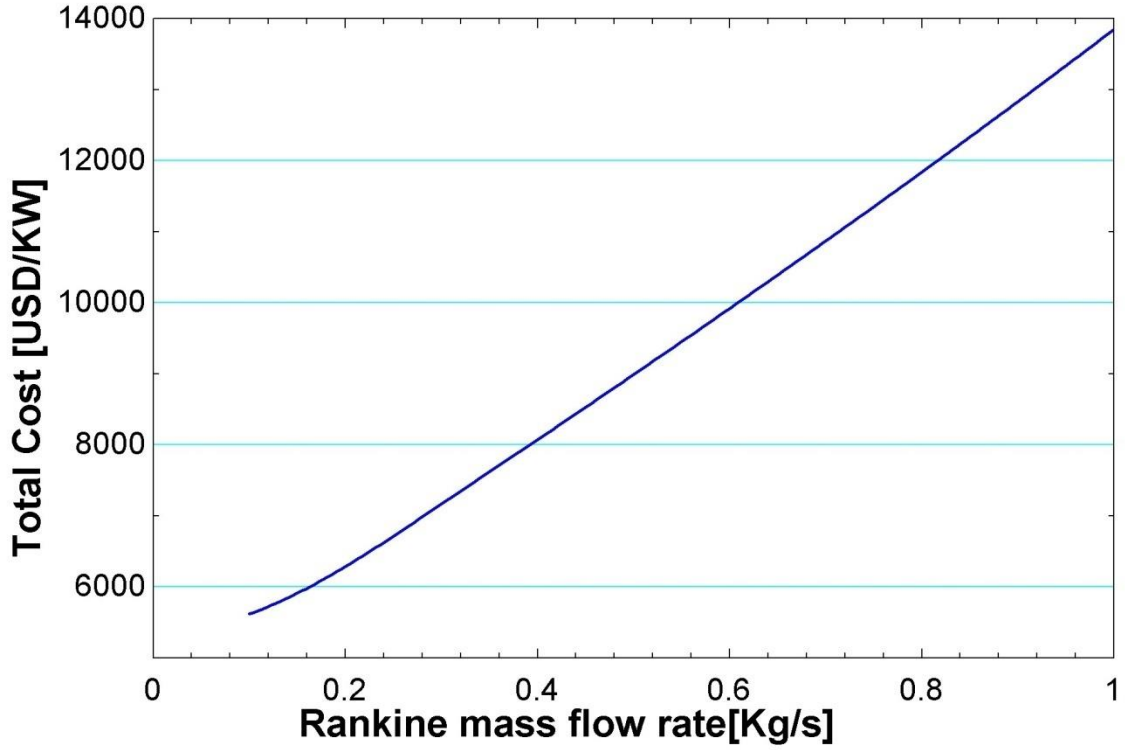

Figure 4.20: Total Cost verses Rankine mass flow rate

Chapter 5

5. Conclusions

Inclusion of an internal heat exchanger in the bottoming cycle is found to be ineffective in waste heat recovery. This is because an internal heat exchanger reduces the amount of heat transfer to the bottoming cycle. The excess heat is then just rejected to the environment which counteracts the whole purpose of including a bottoming power cycle for waste heat recovery. An alternative solution would be to keep the IHX and capture that excess heat with an additional bottoming cycle. Unfortunately, every subsequent bottoming cycle sees diminishing returns and at some point the capital cost outweighs the benefits. A better utilization of exergy is to produce domestic hot water in the condenser.

Improving the topping cycle recuperator effectiveness makes the topping cycle more efficient in the sense that less heat is required from fuel. However, less heat is rejected to the bottoming cycle. A reduction in heat transfer from the topping cycle reduces the net power output of the bottoming cycle. For situations where increasing the recuperator effectiveness is unrealistic, inclusion of a heat recovery bottoming cycle is effective.

For turbine inlet temperature of 1500 K and a combustor inlet temperature of 300 K, a combustor irreversibility of about 30 % is achieved. An increase in the turbine inlet temperature does increase combustor irreversibility but raises the system efficiency.

Increasing the ambient temperature intuitively reduces the overall first and second law efficiency because of a decrease in the Carnot efficiency. Due to carbon dioxide's critical temperature near ambient temperature, the bottoming cycle is more sensitive to change in ambient temperature. The saturation temperature and pressure of carbon dioxide are related to the ambient temperature through the condenser temperature difference. Special attention must be given to the condensation temperature because if it exceeds 31 °C, the heat rejection process because supercritial. This has a primary affect on the bottoming cycle pressure ratio which is related to pump and turbine power.

Increasing the bottoming cycle max pressure increases the energetic efficiency and exergetic efficiency but reduces exergy destruction. The maximum net power occurs at an

extremely high pressure on the order of 110 MPa. Current material properties limit the max pressure to about 20 MPa.

For the configuration studied, a maximum topping cycle net work occurs at a Brayton cycle pressure ratio of 8. Above a pressure ratio of 8, the incremental power increase of the compressor begins to exceed that for the turbine. It should be noted that this is the result for a topping cycle without intercooling and reheat.

Increases of pressure losses within components have two major disadvantages. First, increased pressure loss increases the change in entropy and entropy production. This increase in entropy production translates to exergy destruction. Second, work potential is reduced because the creation of back pressures throughout the cycle reduce expansion ratio in turbines.

By increasing the exhaust temperature from naval ships gas turbine exhaust, it increases the system power output and it also increases the system efficiency. Besides saving of fossil fuel and pollution control also be achieved by this process.

5.2 Scope for future work

In this thesis only simple economic analysis of system occurs. So in future we can do the exergo- economic analysis of system which optimises our results. We can use a internal heat exchanger before waste heat recovery heat exchanger in which hot fluid is coming from Brayton turbine exhaust and cold fluid is coming from pump.

References :

[1]. BCS Inc. *Waste Heat Recovery: Technology and Opportunities in the U.S. Industry*. U.S Department of Energy, 2008

[2]. Kehlhofer, R. *Combined-Cycle Gas and Steam Turbine Power Plants*; Penn Well Publishing Company: Tulsa, Oklahoma, 1997.

[3]. Marrero, I.O.; Lefsaker, A. M.; Razani, A; Kim, K.J. 'Second law analysis and optimization of a combined power cycle'. *Energy Conversion and Management* **2002,** *43*, 557-573.

[4]. Siemens Energy. Combined Cycle site. http://www.energy.siemens.com/us/en/ industries-utilities/power/processes/combined-cycle.htm (accessed 3/31/13).

[5]. Chen, Y.; Lundqvist, P.; Johansson, A.; Platell, P. 'A comparative study of the carbon dioxide transcritical power cycle compared with an organic Rankine cycle with R123 as working fluid in waste heat recovery'. *Applied Thermal Engineering* **2006**, *26*, 2142-2147.

[6]. Kim, M-H.; Petterson, J.; Bullard, C.W. 'Fundamental process and system design issues in CO2 vapor compression systems'. *Progress in Energy and Combustion Science* **2004**, *30*, 119-174.

[7]. Feher, E.G. 'The Supercritical Thermodynamic Power Cycle'. *Energy Conversion* **1968**, *8*, 85-90.

[8]. Wright, S. Mighty Mite. *Mechanical Engineering*, [Online], January, **2012**. http://www.barber-nichols.com/sites/default/files/wysiwyg/images/ supercritical_co2_turbines.pdf (accessed October, 2012).

[9]. Persichilli, M.; Kacludis, A.; Zdankiewicz, E.; Held, T. *Supercritical CO2 Power Cycle Developments and Commercialization: Why sCO2 can Displace Steam*, Proceedings from Power-Generation India & Central Asia Conference, Pragati Maidan, New Delhi India, April 19-21, **2012**.

[10]. Cayer, E.; Galanis, N.; Desilets, M.; Nesreddine, H.; Roy, P. 'Analysis of a carbon dioxide transcritical power cycle using a low temperature source'. *Applied Energy* **2009**, *86*, 1055-1063.

[11]. Velez, F.; Segovia, J.; Chejne, F.; Antolin, G.; Quijano, A.; Martin, M.C. 'Low temperature heat source for power generation: Exhaustive analysis of a carbon dioxide transcritical power cycle'. *Energy* **2011**, *26*, 5497-5507.

[12]. Chen, Y.; Lundqvist, P.; Platell, P. ‘Theoretical research of carbon dioxide power cycle application in automobile industry to reduce vehicle's fuel consumption’. *Applied Thermal Engineering* **2005** , *25*, 2041-2053.

[13]. Austin, B.T.; Sumathy, K. Transcritical carbon dioxide heat pump systems: A review. *Renewable and Sustainable Energy Reviews* **2011**, *15*, 4013- 4029.

[14]. McQuay Air Conditioning. *Refrigerants Application Guide;* Technical Report No. AG 31-007, **2002**.

[15]. Roy, J.P. Mishra, M.K. Misra, ‘A. Parametric optimization and performance analysis of a waste heat recovery system using Organic Rankine Cycle’. *Energy* **2010**, *35*, 5049-5062.

[16]. Velez, F.; Segovia, J.J.; Martin, M.C.; Antolin, G.; Chejn, F.; Quijano, ‘A. Comparative study of working fluids for a Rankine cycle operating at low temperature’. *Fuel Processing Technology* **2012**, *103*, 71-77.

[17]. Vaja, I.; Gamborotta, A. ‘Internal Combustion Engine (ICE) bottoming with Organic Rankine Cycles (ORCs)’. *Energy* **2010**, *35*, 1084-1093.

[18]. Guo et al., ‘Comparision of Carbon dioxide with other working substance’, *Engineering* **2010**, *92*, 32-45.

[19]. Klein, S. A. *Engineering Equation Solver (EES) for Microsoft Windows Operating System: Academic Commercial* Version; F-Chart Software: Madison, WI, **2012** (available on the Web at http://www.fchart.com).

[20]. Cayer, E.; Galanis, N.; Nesreddine, H. ‘Parametric Study and Optimization of a Transcritical Power Cycle Using a Low Temperature Source’. *Applied Energy* **2010**, *87*, 1249-1257.

[21]. Chen, Y.; Lundqvist, P.; Johansson, A.; Platell, P. ‘A comparative study of the carbon dioxide transcritical power cycle compared with an organic Rankine cycle with R123 as working fluid in waste heat recovery’. *Applied Thermal Engineering* **2010**, *26*, 2142-2147.

[22]. Chen, Y.; Lundqvist, P.; Platell, P. ‘Theoretical research of carbon dioxide power cycle application in automobile industry to reduce vehicle's fuel consumption’. *Applied Thermal Engineering* **2005** , *25*, 2041-2053.

[23]. Byung Chul Choi ; Young Min Kim, ‘Thermodynamic analysis of a dual loop heat recovery system with trilateral cycle applied to exhaust gases of internal combustion engine for propulsion of the 6800 TEU container ship’, Energy volume 58**, September, 2013.**

[24]. Min-Hsiung Yang , Rong-Hua Yeh; 'Economic performances optimization of the transcritical Rankine cycle systems in geothermal application', Energy Conversion and Management 95 (**2015**) 20–31.

[25]. Farivar Fazelpour; Tatiana Morosuk, 'Exergo economic analysis of carbon dioxide transcritical refrigeration machines', Department of Energy System Engineering, Islamic Azad University e South Tehran Branch, P.O. Box. 11365.4435, No. 173, Sepahbod Gharani Ave., Teheran, Iran, Institute for Energy Engineering, Technische Universita¨t Berlin, Marchstr 18, 10587 Berlin, Germany , accepted on September, 2013.

[26]. Sylvain Quoilin , Sébastien Declaye , Bertrand F. Tchanche ,Vincent Lemort , 'Thermo-economic optimization of waste heat recovery Organic Rankine Cycles', Thermodynamics Laboratory University of Liège, Campus du Sart Tilman, B49, B-4000 Liège, Belgium Agricultural University of Athens, 75 Iera Odos Street, 11855 Athens, Greece, accepted on may, 2011.

[27]. Mr. Dean Putnam dean.r.putnam@navy.mil, '(SBIR) Navy Gas Turbine Engine Exhaust Waste Heat Recovery Shipboard Module Development' Navy SBIR 2010.3 Topic N103229 on **August 17, 2010**.

[28]. Saili Li, Yiping Dai , 'Thermo-economic comparison of Kalina and CO2 transcritical power cycle for low temperature geothermal sources in China', Institute of Turbomachinery, School of Energy and Power Engineering, Xi'an Jiaotong University, No. 28 Xianning West Road, Xi'an 710049, China